Massive Wireless Multiway Relay Systems Employing Uncoordinated Transmission Scheme

Mohammad Nur Hasan

School of Information Science

Japan Advanced Institute of Science and Technology

March, 2016

Master's Thesis

Massive Wireless Multiway Relay Systems Employing Uncoordinated Transmission Scheme

1410035 Mohammad Nur Hasan

Supervisor : Professor Tad Matsumoto
Main Examiner : Professor Tad Matsumoto
Examiners : Associate Professor Brian Kurkoski
Associate Professor Kiyofumi Tanaka

School of Information Science
Japan Advanced Institute of Science and Technology

February, 2016

I certify that I have prepared this Master's Thesis by myself without any inadmissible outside help.

Mohammad Nur Hasan
JAIST, 10 February 2016

Author : _____

Date : _____

Supervisor : _____

Abstract

Number of connected devices is increasing unprecedentedly that by the year 2020 more than 50 billion devices are connecting to the networks. This situation motivates us in this thesis to develop efficient transmission strategies using multiway relay networks (MWRN) to serve *massive* number of devices (users) as solutions for the massive connection challenges.

First, this thesis studies very simple case of MWRN, where a single relay terminal is employed to help users to fully exchange information among themselves, termed as *multiway single relay networks* (MWSRN). To date, MWSRN is proposed with fixed transmission scheduling that inherits high complexity when the number of users is very large. To solve this problem, this thesis proposes uncoordinated transmission (random access) strategy, where the users are allowed to transmit their information (messages) randomly to the networks, and hence, no transmission scheduling is required. Conventionally, uncoordinated transmission suffers from low throughput performance due to the fact that the collided messages are discarded. Contrarily, in this works, instead of avoiding the collision, we exploit the collided messages using successive interference cancellation (SIC) to improve throughput performance. This thesis further proposes iterative demapping (IDM) algorithm to be incorporated into SIC to achieve networks throughput beyond $T = 1$ packet/slot, which is the limit of the conventional random access throughput.

This thesis shows that the proposed uncoordinated transmission strategy in MWSRN resembles a coding structure similar to low-density parity-check (LDPC) codes structure that can be represented by a bipartite graph. Accordingly, the similar analysis techniques, extrinsic information transfer (EXIT) analysis, which is basically for physical layer, is utilized to analyze the decoding convergence behavior of the networks. The network capacity bound expressing maximum offered traffic that can be reliably handled by the networks is derived based on EXIT chart area theorem. It is shown that with IDM algorithm the proposed MWSRN has two times higher bound compared to the conventional MWSRN, which also implies that throughput of $T = 2$ packets/slot is *asymptotically* achievable using the proposed technique. The computer simulation results confirm the superiority of the proposed techniques in terms of throughput and packet-loss-rate (PLR) performances. In practice, the proposed MWSRN can achieve throughput greater than $T = 1$ packet/slot. It also offers very low PLR floor because the probability

of degree-two stopping set can be eliminated by employing IDM algorithm in SIC.

The rest of the thesis focuses on the extension of MWSRN to serve wider and larger network coverage by proposing multiple relays, called *multiway multirelay networks* (MWMRN). The uncoordinated transmission strategy is adopted in multiple access channel (MAC) phase. The relays decode all received messages using the proposed IDM-based SIC, yielding significant performance improvement in MAC phase. The decoded messages in the relays are correlated since they are originally sent from the same source. Joint decoding that exploits the correlation of messages in the relays is proposed to achieve excellent performances. In the final step of joint decoding, the selection of *host decoder*, of which the outputs are used for finals decision, is of significant importance to obtain the best decoding results. This thesis solves *host decoder selection* problem using mutual information calculated by the relays. The results of computer simulations show that the proposed techniques outperform the conventional techniques in terms of throughput and bit-error-rate (BER) performances. It is also confirmed that $Q \in \{1, 2\}$ are the practical optimal numbers of relays in terms of throughput or BER performances for MWMRN with randomly distributed users. All findings in this thesis are expected to solve the future massive networking problems by the year 2020.

Keywords: Multiway Relay Networks, Multiway Multirelay Networks, Uncoordinated Transmission, Graph-based Successive Interference Cancellation, Joint Decoding, Iterative Demapping Algorithm, Source Correlation.

Acknowledgments

First of all, I am grateful to the Almighty God, Allah SWT, for the wisdom that He has been bestowed upon me during the master research, and indeed, throughout my life.

I am deeply grateful to Professor Khoirul Anwar for allowing me to join his research project that becomes the core of this thesis. I am grateful to him for his patient guidance, suggestions, inspirations, and encouragement throughout my master research. Without his knowledge, guidance, and selfless assistance this thesis would not have been completed. I feel so blessed to be included in your group since you provide me so much support, friendship, and warm encouragement. May Allah gives you the best reward for that.

I would like to express my sincere gratitude to my formal academic supervisor, Professor Tadashi Matsumoto, for providing an opportunity to work in his group, his support, and encouragement during the course of my research work.

I would like to express my gratitude to my supervisor committee, Professor Brian Kurkoski and Professor Kiyofumi Tanaka, for their insightful comments and valuable suggestions. Especially for Professor Brian Kurkoski, I still need your support during the doctoral starting from this April. I hope we can work together in harmony and make a lot of contribution in our research field.

I also take this opportunity to record my sincere thanks to all members of Information Theory and Signal Processing Laboratory for their supports and warm friendship throughout my research period.

In addition, I would to express the deepest appreciation to the Japan Society for the Promotion of Science (JSPS) KAKENHI KIBAN KENKYU (B) Grant No. 25289113 and Docomo International Student Scholarship for providing me financial support to carry out the research.

Finally, I am thankful to my dearest wife Dian Novitasari for her unconditional love and continuous support and my son Rizqi Haikal Hasan who always converts my tiredness to become happiness when I returned from work. It was because of my wifes effort to encourage me to pursue my dream and get an academic degree in Japan. I am really blessed with her presence. I dedicated this work to my parents for their encouragement, pray, and support throughout my life.

Table of Contents

List of Figures

List of Tables

Abbreviations

ACC	Doped-Accumulator
AWGN	Additive White Gaussian Noise
BER	Bit Error Rate
BPSK	Binary Phase Shift Keying
CRDSA	Contention Resolution Diversity Slotted ALOHA
CSA	Coded Slotted ALOHA
D	Decoder of convolutional codes
DACC	Decoder of ACC
DM	Demapper
D-MWMRN	Multiway Multirelay Networks with Distributed Users
EXIT	Extrinsic Information Transfer
FER	Frame Error Rate
HI	Horizontal Iteration
IC	Interference Cancellation
IDM	Iterative Demapping
IRSA	Irregular Repetition Slotted ALOHA
LLR	Log Likelihood Ratio
MAP	Maximum a Posteriori
MI	Mutual Information
MPR	Multipacket reception

MTD	Machine-type-device
MWRN	Multiway Relay Networks
MWMRN	Multiway Multirelay Networks
MWMRN-2C	Multiway Multirelay Networks with Two Clusters
MWSRN	Multiway Single Relay Networks
PLR	Packet Loss Rate
pmf	Probability Mass Function
PTS	Pair of Time Slot
SA	Slotted ALOHA
SCC	Serial Concatenated Code
SIC	Successive Interference Cancellation
SNR	Signal-to-Noise Power Ratio
TS	Time Slot
VI	Vertical Iteration
VN	Variable Node

Notations

A	Transmission matrix received by relay
A_i	Transmission matrix received by user u_i
B	Amplification factor of AF relay
$\mathcal{C}$	Set of *network* encoders
c_h	*Network* encoder (h, k)
d	Degree of slot nodes
ϵ	Correlation factor of messages
$\mathcal{E}$	Set of edges in bipartite graph
G	Offered traffic
G^*	Threshold of offered traffic
G_{BC}	Offered traffic in BC phase
G_{MAC}	Offered traffic in MAC phase
$\mathcal{G}$	Bipartite graph corresponding to uncoordinated transmission scheme
γ	Pathloss exponent
$\Gamma_{a,b}$	SNR from point a to point b
h	Code length of *network* encoder c_h or degree of user nodes
$\overline{h}$	Expected length of *network* encoders
i	Index of users
j	Index of slots (TS or PTS)
k	Number of Information Blocks

$\mathcal{K}$	Length of data b_i
L	Frame length in MWMR networks
$\mathcal{L}$	Number of the reliable LLRs
Λ	Probability mass function of *network* encoders
Λ_h	Probability of network encoder c_h is chosen
λ_h	Probability of an edge belongs to user node type h
$\lambda(x)$	Degree distribution of user nodes from edges perspective
ℓ	Iteration index in the iterative decoding
M	Number of users
N	Length of uncoordinated transmission frame
n_c	Maximum code length of *network* encoder
p	Probability of an edge carrying erasure message from slot node to user node
P	Transmit power
$\Psi(x)$	Degree distribution of slot nodes from nodes perspective
q	Probability of an edge carrying erasure message from user node to slot node
Q	Number of relays
R_N	Average rate of *network* encoder per user
R_h	Rate of *network* encoder in a user selecting c_h
R_P	Rate of physical encoder
$\mathcal{R}_r$	r-th relay
ρ_d	Probability of an edge belongs to slot node type d
$\rho(x)$	Degree distribution of slot nodes from edges perspective
$\mathcal{S}$	Set of slots or *slot nodes*
σ^2	Noise variance
T	Throughput
$T_{\max}$	Maximum throughput
$\mathcal{T}$	Threshold of reliable LLR
$\mathcal{U}$	Set of users or *user nodes*

Chapter 1

Introduction

1.1 Background and Motivation

Since the introduction of Internet of Things (IoT) concept, the number of connected devices (*things*) is rapidly increasing. The devices are not limited to smart phones or computers, but the other *things* like houses, cars, sensors, and other machine-type-devices (MTD), will also be connected to the networks. The connections of these *things* will deliver great impacts on many areas such as education, communication, bussiness, science, goverment, and humanity. Fig. 1.1 illustrates the prediction that by 2020, there will be more than 50 billion connected devices, which is 6.58 times higher than the world population [1] [2]. This condition is in tune with next fifth generation networks, 5G, where ultra-dense networks is one of the major challenges. In this situation, an efficient wireless communication strategy that can handle massive number of devices (users) is highly required.

We consider multiway relay networks (MWRN) [3] as one of potential solutions for future networks because of its superiority in serving multiple users. MWRN has attracted a considerable attention and has been extensively studied, for example, in [3] [4], and [5]. However, in the literature, MWRN is only proposed with fixed transmission scheduling, which naturally inherits high complexity when number of users is huge. This is because coordination among the users is required in fixed transmission scheduling.

A transmission strategy without perfect coordination is more favorable for communication among massive number of users. Therefore, we propose the employment of uncoordinated transmission (random access) scheme for MWRN. In this

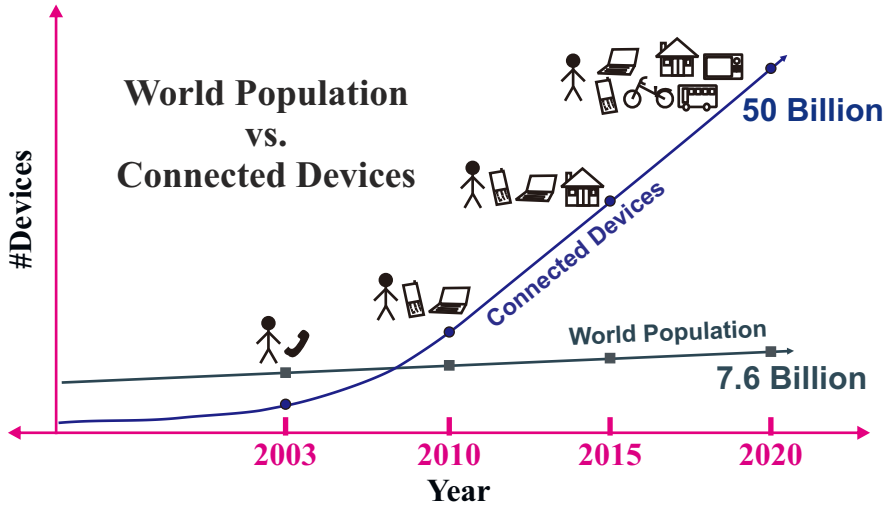

Fig. 1.1: The challenge of future networks: more than 50 billion devices require connection by 2020.

scheme, the users are allowed to transmit their information randomly to the networks, hence the scheduling complexity is significantly reduced. Unfortunately, the traditional random access scheme exhibits low throughput. When several users transmit simultaneously in the same time slots (TS), the messages are collided and cannot be resolved. This collision problem is the main cause of low throughput in random access.

Conventionally, throughput of random access is limited to $T = 1$ packet/slot, for example, traditional slotted ALOHA (SA) only achieves maximum throughput of 0.367 packets/slot. Motivated by this fact, several techniques have been developed to improve the throughput of traditional random access. Diversity slotted ALOHA (DSA) [6] is the first technique that introduces message repetition in random access, yielding a slight throughput improvement with respect to SA. Contention resolution diversity ALOHA (CRDSA) [7] proposes interference cancellation (IC) for resolving the collisions in DSA. This technique achieves throughput up to 0.55 packets/slot, which is a remarkable improvement compared to the SA. In [8], irregular repetition slotted ALOHA (IRSA) was introduced to provide a further throughput gain over CRDSA. It allows the users to irregularly repeat the transmission. The number of repetition is drawn randomly from a designed probability mass function (pmf). Successive interference cancellation (SIC) is adopted

to successively resolve the collided messages, resulting significant throughput improvement asymptotically to 0.97 packets/slot. This technique is then generalized in coded slotted ALOHA (CSA) [9] by using more general *packet-oriented* linear codes, instead of repetition codes. This technique asymptotically achieves throughput $T = 1$ packet/slot using very low rate codes.

Motivated by insights of multiuser detection (MUD) employment in random access given in [10], we propose a novel technique to improve the throughput of uncoordinated transmission beyond the limit of $T = 1$ packet/slot. Particularly, iterative demapping (IDM) algorithm [11], which is capable of decoding two messages simultaneously, is incorporated into graph-based SIC to increase the probability of successful decoding, exhibiting significant throughput enhancement. Adoption of the proposed uncoordinated transmission strategy is also beneficial for MWRN networks to handle massive number of users with heterogeneous traffics. Each users may choose different codes with various rate based on its own traffic for accessing the networks randomly.

In practice, users have random locations in an area. Furthermore, when number of users is very huge, they might be randomly located in a wider and larger area. In this instance, it is natural to employ multiple relays for serving all users with better performances. Because the messages are sent from the same sources, the messages received by the relays are correlated, of which the correlation can be exploited to achieve remarkable performances using a joint decoding. However, what is the optimal number of relays remains as an interesting open problem.

These facts motivates us to conduct this research with aims to: (i) design an efficient MWRN serving massive number of users with throughput $T \geq 1$ packet/slot, (ii) design an effective decoding for MWRN exploiting correlated sources, and (iii) analyze the optimal number of relays required in MWRN with distributed users.

1.2 Research Contribution

The contributions of this research are summarized as follows:

- We propose uncoordinated transmission scheme in MWRN for serving massive number of users. Since complex coordination among huge number of users during transmission is not required, the transmission scheduling design is very simple.

- We propose a novel decoding technique for uncoordinated transmission using graph-based SIC with IDM algorithm, resulting throughput improvement beyond $T = 1$ packet/slot.
- We derive the theoretical network capacity bound expressing maximum offered traffic that can be reliably handled by the networks using EXIT chart area theorem. This bound confirms that the proposed techniques can asymptotically achieve throughput of $T = 2$ packets/slot.
- We enlarge the networks coverage by employing multiple relays and exploit source correlation existing in the networks. The final joint decoding is proposed to exploit the source correlation of the decoded messages in the relays. We also propose the selection of *host decoder*, of which the outputs are used for final decision, based on mutual information (MI) to ensure the best decoding results.
- We analyze the optimal number of relays to efficiently serve massive number of users randomly distributed in an area.

1.3 Thesis Outline

This thesis is organized as follows.

In **Chapter 1** (this chapter), we describe the background and motivation of the research. We also summarize the contribution of the research and present the thesis outline.

In **Chapter 2**, we discuss some fundamental concepts, techniques, and algorithms used in this research for better understanding the main part of this thesis.

In **Chapter 3**, we explain the motivations of two system models considered in this thesis: *multiway single relay networks* (MWSRN) and *multiway multirelay networks* (MWMRN).

In **Chapter 4**, we work on uncoordinated transmission in MWSRN, which is the simplest MWRN scenario. We analyze the proposed decoding strategy and its convergence behavior using EXIT analysis. We also derive the network capacity bound of the proposed uncoordinated transmission scheme.

In **Chapter 5**, we then extend the networks using multiple relays, known as MWMRN. We consider two cases of MWMRN. The first case is when there are

two relays serving two clusters of users. The second case is more general scenario, where arbitrary number of relays are employed to serve massive number of users randomly distributed in an area. We propose joint decoding strategy to remarkably improve the network performances.

In **Chapter 6**, we present conclusions of the thesis. Some insights into the future works are also provided.

Chapter 2

Preliminaries

In this chapter, we briefly provide introduction and explanation of the background knowledge, coding and decoding techniques, and algorithm utilized in this research. Firstly, we introduce the concept of relay networks. We then describe the idea of SIC, which is one of the important decoding strategies in the proposed uncoordinated transmissions. We continue by explaining the serial concatenated convolutional (SCC) codes, which are used as the channel encoder in the following chapters. Finally, the IDM algorithm that is capable of decoding two messages simultaneously is briefly described.

2.1 Relay Networks

Relaying strategy was initially proposed to help a source transmitting information to destination via unreliable channel. This strategy is then developed as cooperative communications that offers higher spectrum efficiency and diversity. There are three main relay networks models. Fig. 2.1(a) illustrated the first model, unidirectional relay networks. In this networks, a source wants to send information to a destination with the help of relay [12] [13] in one direction. The unidirectional relay networks is then extended to bidirectional or two-way relay networks, where two users are communicating in two directions with the help of the relay [14] [15] as shown in Fig. 2.1(b). This thesis focuses on the third relay networks model, multiway relay networks (MWRN) as shown in Fig. 2.1(c). MWRN consists of multiple users who expect to exchange information among themselves with the help of the relay.

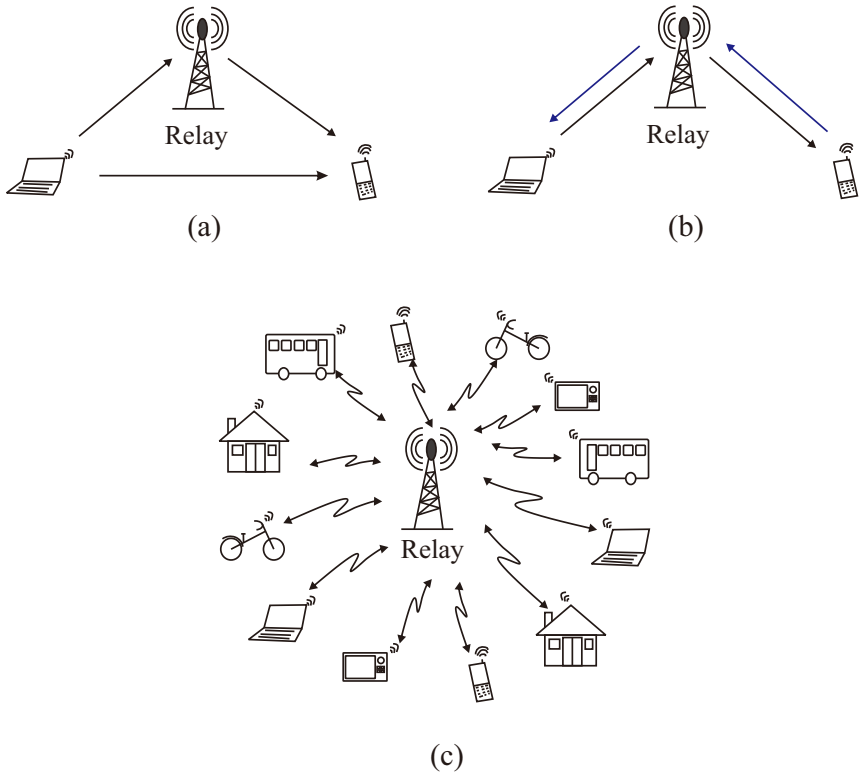

Fig. 2.1: Relay networks models: (a) unidirectional relay networks, (b) two-way relay networks, and (c) multiway relay networks.

Since its introduction in [3], MWRN has attracted a considerable attention owing to its potential applications. The examples of applications include super-dense networks, quickly built devastated networks, wireless sensor networks, and satellite networks. This networks is also regarded as one potential solution of the future networks, where massive number of devices need connection to the networks.

2.2 Successive Interference Cancellation

Interference is usually regarded as a highly undesired problem. Since the number of devices (transmitters) is exponentially increasing, interference is almost impossible to avoid. Successive interference cancellation (SIC) is a clever technique to treat the interference problem involving massive number of users. First introduced in [16], the main concept of SIC is to decode all the users sequentially. Before decoding the other users, the interference caused by the decoded users is subtracted.

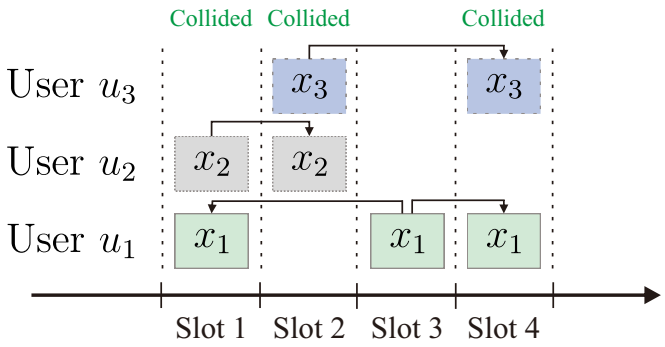

Fig. 2.2: SIC in random access.

For example, when two or more users transmit messages simultaneously to a common destination, the stronger signal is first decoded. The decoded messages are then reconstructed and subtracted from the combined signal. The same process is iteratively performed for the *residue* signal to decode all the messages, hence it is termed *successive interfere cancellation* or *capture effect*.

Recently, SIC is adopted to random access technology and becomes a major breakthrough for throughput enhancement. It enables the collisions (interference)[1] to be favorably exploited instead of being regarded merely as a useless. The interference caused by the collided messages in a slot is canceled using the copy of the message successfully decoded in another slot. Fig. 2.2 shows the example of SIC in random access, where user u_1 transmits the same messages in slots 1, 3, and 4, user u_2 in slots 1 and 2, while user u_3 transmits via slots 2 and 4. In the conventional random access decoding, only message x_1 transmitted via slot 3, where no collision occurs, can be correctly decoded. Employing the SIC, the decode messages x_1 is reconstructed to subtract the other messages of user u_1 in slots 1 and 4. Accordingly, the both messages x_2 and x_3 can also be correctly resolved by the same process.

2.3 Serial Concatenated Convolutional Codes

Serial concatenated convolutional (SCC) codes are developed extending the idea of Turbo codes, which was first introduced in 1993 as the first practical codes

[1]Collision and interference are used interchangeably in this thesis.

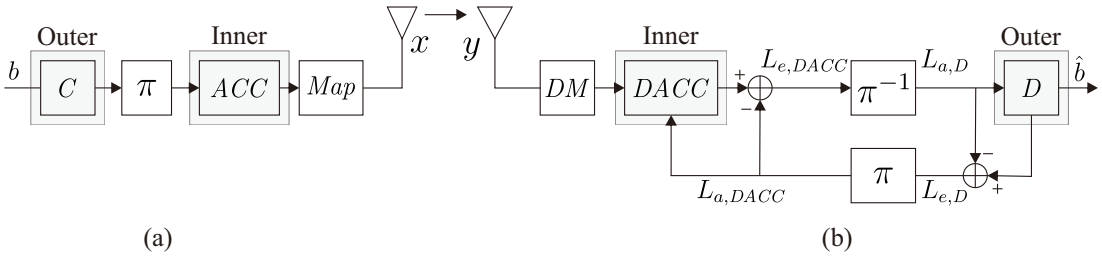

Fig. 2.3: Encoding and decoding blocks of serial concatenated convolutional (SCC) codes considered in this thesis.

that can asymptotically achieve the Shannon-limit. The encoding blocks of SCC constructed by serial concatenation of two convolutional codes as *inner* and *outer* codes are shown in Fig. 2.3(a). To support future networks with low complexity, this thesis uses very simple convolutional codes. Memory-1 $[3, 2]_8$ convolutional codes with half rate are employed as the *outer* codes C. While for the *inner* codes, we utilize doped-accumulator (ACC) [17] [18], which is memory-1 convolutional codes with unity rate. The *inner* and *outer* codes are separated by an interleaver π to make the two encoded bit sequences statistically independent.

Fig. 2.3(b) describes the decoding structure of SCC performed iteratively between two component decoders, D and $DACC$ as decoders of C and ACC, respectively. Soft information is exchanged between two decoders in the form of *extrinsic* log-likelihood ratio (LLR) defined as:

$$L_e(b) = \ln\left[\frac{\Pr(y|b=0)}{\Pr(y|b=1)}\right] \tag{2.1}$$

with the corresponding deinterleaver π^{-1} and interleaver π. In each decoder, soft decoding is performed using Bahl-Cocke-Jelinek-Raviv (BCJR) algorithm. The outputs of each decoder are *a posteriori* LLRs,

$$L_p(b) = \ln\left[\frac{\Pr(b=0|y)}{\Pr(b=1|y)}\right], \tag{2.2}$$

which are then subtracted by *a priori* LLRs,

$$L_a(b) = \ln\left[\frac{\Pr(b=0)}{\Pr(b=1)}\right], \tag{2.3}$$

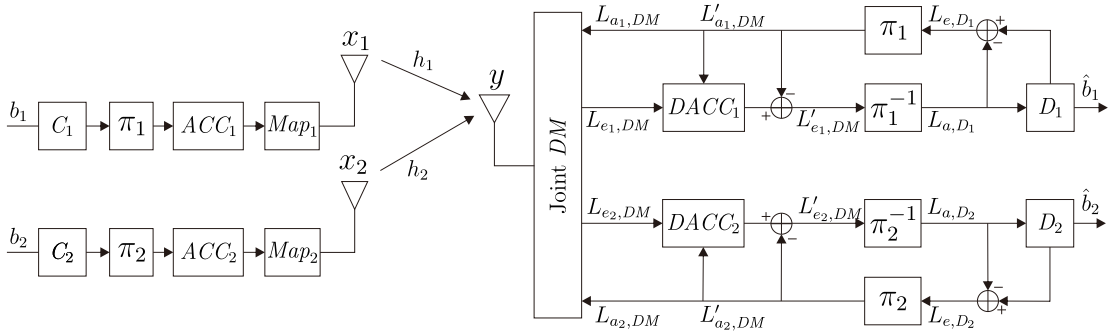

Fig. 2.4: IDM algorithm that can decode two messages simultaneously.

resulting extrinsic LLRs, $L_e(b)$. Final decision is then performed at the end of iteration based on $L_p(b)$ producing $\hat{b}$.

2.4 Iterative Demapping Algorithm

Iterative demapping (IDM) algorithm was introduced in [11] for three-way relaying systems. This technique has capability of decoding messages from two users simultaneously. Fig 2.4 explains how IDM algorithm works as an extension of SCC. Users u_1 and u_2 want to deliver *binary* data b_1 and b_2, respectively, to a common destination. Each user encodes the data using SCC codes and maps them to symbols x_i. For simplicity, we assume x_i is a binary phase shift keying (BPSK) symbol having $E[|x_i|^2] = 1$. An extension to higher order modulation is rather straightforward. Both users transmit messages x_1 and x_2 in the same time, and thus, the destination receives

$$y = h_1 x_1 + h_2 x_2 + z, \tag{2.4}$$

where h_i is channel gain from user u_i and z is additive white Gaussian noise (AWGN) with variance σ^2.

Decoding process in the destination consists of a joint demapper (DM) and two independent turbo loops involving decoders D_i and $DACC_i$ the decoding of which is similar to that of SCC codes. With the help of *a priori* LLR from decoder D_1,

$L_{a_1,DM}$, joint DM calculates extrinsic LLR $L_{e_2,DM}$ of symbol x_2 as

$$\begin{aligned} L_{e_2,DM} &= \ln \frac{\Pr(x_2 = +1|y)}{\Pr(x_2 = -1|y)} \\ &= \ln \frac{\sum_{\mathcal{X} \in \mathcal{X}_{x_{2+}}} \exp\left\{ -\frac{|y - h_1 x_1 - h_2 x_2|^2}{\sigma^2} - b_1 L_{a_1,DM} \right\}}{\sum_{\mathcal{X} \in \mathcal{X}_{x_{2-}}} \exp\left\{ -\frac{|y - h_1 x_1 - h_2 x_2|^2}{\sigma^2} - b_1 L_{a_1,DM} \right\}}, \end{aligned} \tag{2.5}$$

where $\mathcal{X}_{x_{2+}}$ and $\mathcal{X}_{x_{2-}}$ are sets of superposition symbols having symbol x_2 being $+1$ and -1, respectively, with $x_2 = 1 - 2b_2$. Similarly, the calculation of extrinsic LLR $L_{e_1,DM}$ of symbol x_1 by the joint DM is given by

$$\begin{aligned} L_{e_1,DM} &= \ln \frac{\Pr(x_1 = +1|y)}{\Pr(x_1 = -1|y)} \\ &= \ln \frac{\sum_{\mathcal{X} \in \mathcal{X}_{x_{1+}}} \exp\left\{ -\frac{|y - h_1 x_1 - h_2 x_2|^2}{\sigma^2} - b_2 L_{a_2,DM} \right\}}{\sum_{\mathcal{X} \in \mathcal{X}_{x_{1-}}} \exp\left\{ -\frac{|y - h_1 x_1 - h_2 x_2|^2}{\sigma^2} - b_2 L_{a_2,DM} \right\}}. \end{aligned} \tag{2.6}$$

The $DACC_i$ uses extrinsic LLR $L_{e_i,DM}$ and *a priori* LLR $L'_{a_i,DM}$ to produce extrinsic LLR $L'_{e_i,DM}$ that is then deinterleaved by π_i^{-1} and used as inputs of decoder D_i. Final decision is performed after enough iterations based on *a posteriori* LLRs form D_1 and D_2 producing $\hat{b}_1$ and $\hat{b}_2$, respectively.

2.5 Summary

In this chapter, we have introduced some fundamental concepts, coding and decoding techniques, and algorithm used in this thesis. First, we introduced relay networks, and then followed by explanation of SIC. The SCC codes and IDM algorithm are also briefly described. This preliminaries will help readers to smoothly understand the main part of the thesis.

Chapter 3

System Models

This chapter mainly focuses on describing system models considered in this thesis and their motivations. There are two main system models under consideration. The first is the basic MWRN model consisting of multiple users and a *single* relay terminal. Thereby, it is termed as *multiway single relay networks* (MWSRN) in this thesis. The second is a more general model of MWRN, where *multiple* relays are considered to facilitate information exchange among multiple users. Accordingly, it is termed as *multiway multirelay networks* (MWMRN) in this thesis.

This research is in tune with the connected devices development as introduced in [2], where in the future, billions of devices are connected to the networks. Fig. 3.1 shows three waves expressing application models of billion connected devices. The first wave is *networked consumer electronics*, where mostly customer electronics *things* such as phones, computers, refrigerators, TVs, and other MTDs in home, are connected to the networks. The second wave is *networked industries*, where the *things* from industries sector such as trucks, factory machines, solar cells, and other MTDs used in industries, are also connected. Finally, the third wave is *networked everything*, in which all the *things* including humans and society are connected to the networks.

This thesis considers system models representing the three waves of future connected devices shown in Fig. 3.1. The first system model, MWSRN, represents first wave, *networked consumer electronics*, while the second system model represents the second wave, *networked industries*, and third wave, *networked everything*.

For the sake of simplicity, this thesis only considers devices or users with no mobility, which allow us to investigate the networks under AWGN channels assump-

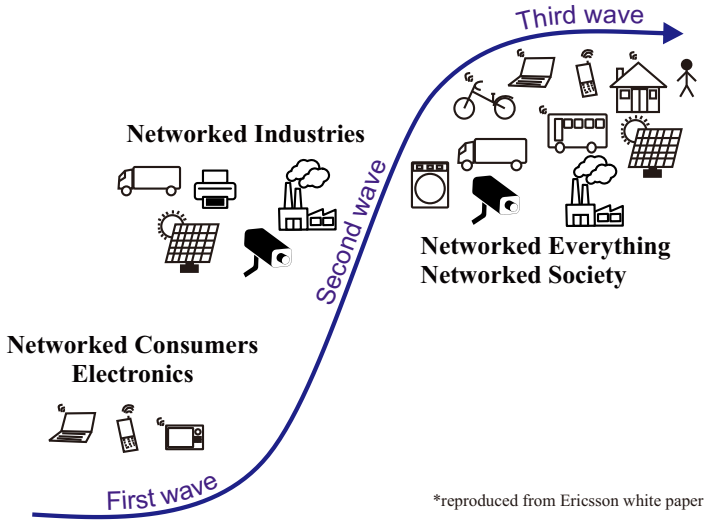

Fig. 3.1: Three waves showing application models of connected devices.

tion. For the case of devices with mobility, implying Rayleigh fading channels, it has been extensively investigated, for example, in [19–21].

3.1 Multiway Single Relay Networks

This thesis first studies MWSRN, the topology of which is very simple as shown in Fig. 3.2. The users have connection to the relay forming star topology, while direct link between any users is assumed to be neither available nor exploited. This model is very suitable for the first wave development, when customer electronics in home are connected to the networks. However, this model is also applicable for disaster areas networks or satellite communication systems.

The focus of this model is the introduction of uncoordinated transmission scheme for MWRN with single relay terminal. With this simplest model, uncoordinated transmission strategy is easy to explain, especially, when AF relaying protocol is employed. The received messages are immediately amplified and forwarded to all users by the relay, implying that one transmission from a user to other users via the relay can be regarded as one slot. Thus, it is quite straightforward to employ uncoordinated transmission in MWSRN.

We will clearly describe the proposed decoding strategy for uncoordinated transmission that can break the limit of conventional random access throughput.

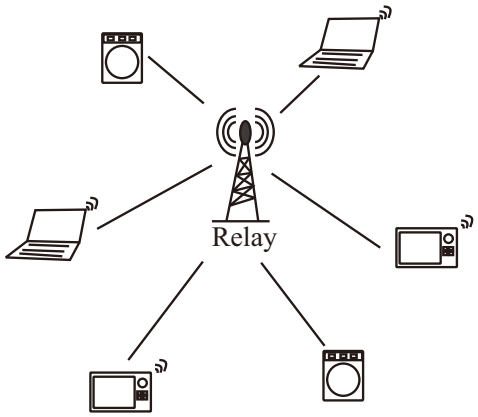

Fig. 3.2: Multiway single relay networks (MWSRN).

The similarity between networks and coding structures of LDPC is also exploited. The density evolution will be used to analyze the convergence behavior of the networks.

3.2 Multiway Multirelay Networks

In the second and third waves of connected devices development, number of devices is tremendously increasing. In this case, it is very natural to employ multiple relays to facilitate massive number of users communicating each other. Multiway multirelay networks (MWMRN) is the extension of MWSRN, where multiple relays are considered.

Two different scenarios of MWMRN are investigated. First, we investigate MWMRN with two clusters of users as illustrated in Fig. 3.3(a). We assume that multiple users are divided into two groups and located in two separated areas with one relay terminal each. All users want to exchange information among themselves with the help of the relays. The practical situations of this scenario are, for examples, wireless communication among devices in two different floors, or two different buildings. In this scenario we focus on mutual information (MI)-based joint decoding strategy that exploits correlation of the messages decoded by the relays to improve the network performances.

We consider more practical situation in the second scenario of MWMRN. The

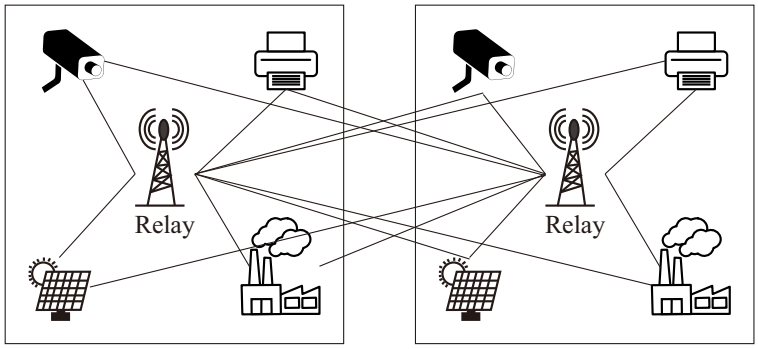

(a)

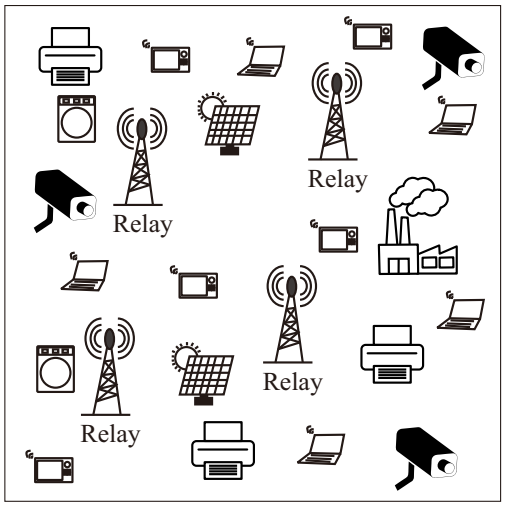

(b)

Fig. 3.3: Multiway multirelay networks (MWMRN) with: (a) two clusters and (b) distributed users.

massive number of users are randomly located or distributed in an area. Arbitrary number of relays are employed to help information exchange among the users. This situation corresponds to the third wave of connected devices development, where various *things* are connected to the networks. In the multiple access channel (MAC) phase, we propose IDM algorithm to be incorporated into graph-based SIC to effectively decode the messages transmitted uncoordinatedly. In the broadcast channel (BC) phase, we generalize the MI-based joint decoding for arbitrary numbers of relays.

3.3 Summary

In this chapter, we have explained the background of system models considered in this thesis. Basically, there are two system models under consideration. First, MWRN with a *single* relay terminal serving massive number of users, called *multiway single relay networks* (MWSRN), is utilized to investigate the fundamental MWRN employing uncoordinated transmission. Second, an MWRN model employing *multiple* relays, known as *multiway multirelay networks* (MWMRN), is considered to investigate more general cases of MWRN with uncoordinated transmission. More technical details will be explained in **Chapters 4** and **5**.

Chapter 4

Multiway Single Relay Networks

In this chapter, we focus on MWRN with a single relay terminal, i.e., MWSRN, aiming to increase throughput beyond $T = 1$ packet/slot. First of all, we provide a brief description of system model of MWSRN under consideration. Then, we introduce uncoordinated transmission scheme that allows massive number of users to randomly transmit their information. We then propose a novel decoding strategy for uncoordinated transmission in MWSRN with capability of decoding multiple messages simultaneously. We also present an asymptotic analysis for the proposed decoding technique and show the derivation of the capacity bound of the system. Finally, simulation results are presented to show the superior performances of the proposed technique.

4.1 System Model

The model considered in this section is shown in Fig. 4.1, where $(M + 1)$ users want to exchange information among themselves with the help of a relay terminal. Each user wants to decode information from the other M users. In this model, it is assumed that there is no direct link between any users, i.e., the users do not receive signals directly from other users except from the relay. This assumption is reasonable for some physical restrictions among the users, e.g., long physical distances, mountainous areas, or high buildings environments.

We consider half-duplex relaying system, which is simple to implement. In the half-duplex case, the information is exchanged within two phases. First phase is multiple access channel (MAC) phase, when some users transmit information

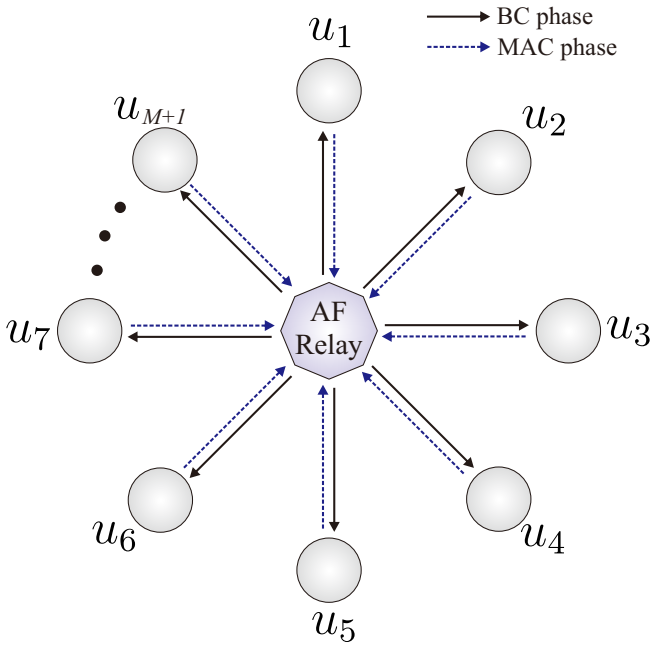

Fig. 4.1: Multiway single relay networks (MWSRN) with AF protocol.

simultaneously to the the relay without coordination with other users. The second phase is broadcast channel (BC) phase, when the relay broadcasts the received information to all users. For the sake of simplicity, in this model, we employ the amplify-and-forward (AF) protocol.

4.2 Uncoordinated Transmission Strategy

A MAC phase is always followed by a BC phase, where the relay always amplifies and forwards (broadcasts) the messages to all users. Thereby, both time slots (TSs) used for MAC and BC phases can be seen as one *pair-of-time slots* (PTS). Particularly, j-th PTS consists of two consecutive TSs, i.e., $(2j-1)$-th and $(2j)$-th TSs, $j = \{1, 2, ..., N\}$. The information exchange among users is performed within one *frame* composed of N PTSs.

Fig. 4.2 describes transmitter structure of a user in MWSRN. Each user encodes k data (information) using *network* encoder with rate R_h and chooses PTSs randomly for transmission. Prior to transmission, the outputs of *network* encoder are again encoded using *physical* encoder with rate R_P and mapped to binary phase shift keying (BPSK) symbols.

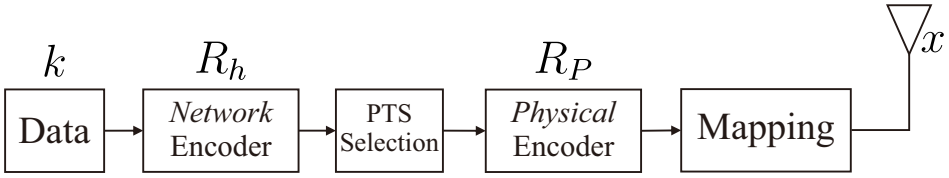

Fig. 4.2: Transmitter structure of a single user.

Technically, each user randomly selects a type of *network* encoder $c_h \sim (h, k)$ from set of *packet-oriented* linear codes $\mathcal{C} = \{c_1, c_2, ..., c_h, ..., c_{n_c}\}$ according to a probability mass function (*pmf*) $\Lambda = \{\Lambda_1, \Lambda_2, ..., \Lambda_{n_c}\}$, where $\sum_{h=1}^{n_c} \Lambda_h = 1$, to encode k information data. A code c_h is a *packet-oriented* linear code with length h, dimension k, and rate $R_h = k/h$. The code length h indicates how many transmissions or PTSs are required to convey the messages to the network. The average rate of *network* encoder, by assuming the same k for each user, is defined as

$$R_N = \frac{k}{\overline{h}}, \tag{4.1}$$

where

$$\overline{h} = \sum\nolimits_{h=1}^{n_c} \Lambda_h h \tag{4.2}$$

is the expected length of *network* codes. The h packets are then transmitted via h randomly selected PTSs. We provide illustration of *network* encoding process and PTS selection in Fig. 4.3. Users u_1, u_3, and u_4 choose $(3, 1)$ codes (repetition codes) as *network* encoder to encode their $k = 1$ data. While user u_2 encodes its data using $(2, 1)$ codes. All users then randomly select PTSs to transmit their encoded packets. For instance, user u_1 randomly chooses PTSs 1, 3, and 4 to transmit the packets.

Prior to transmission, the outputs of *network* encoder are encoded again using *physical* encoder, which is equivalent to channel encoder. In this works, we use SCC codes as *physical* encoder. Subsequently, the encoded packets are mapped to symbol x, which is a BPSK symbol. From networks perspective, the transmission process is illustrated in Fig. 4.4.

We define normalized offered traffic delivered to every user as

$$G = \frac{kM}{N}. \tag{4.3}$$

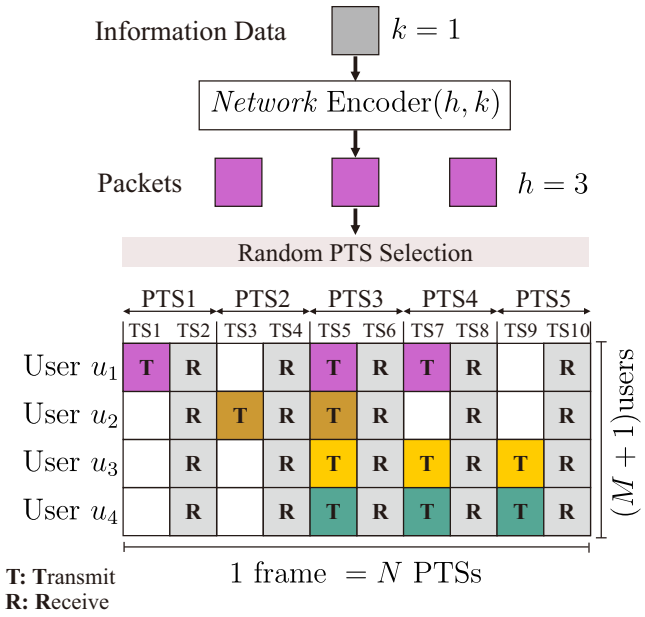

Fig. 4.3: *Network* encoder and PTS selection.

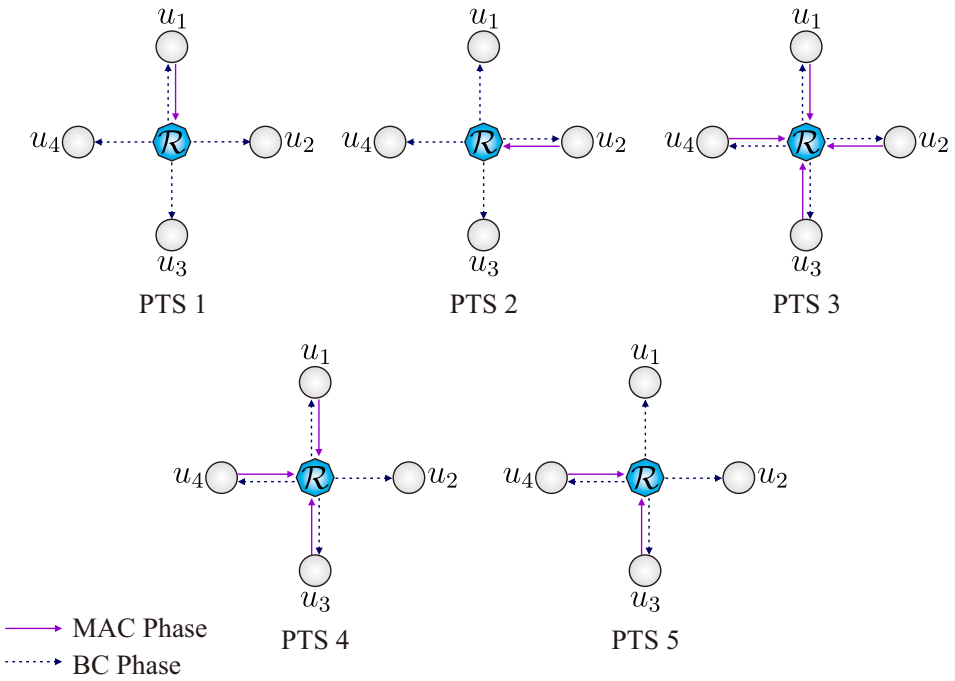

Fig. 4.4: Illustration of transmission process from networks perspective.

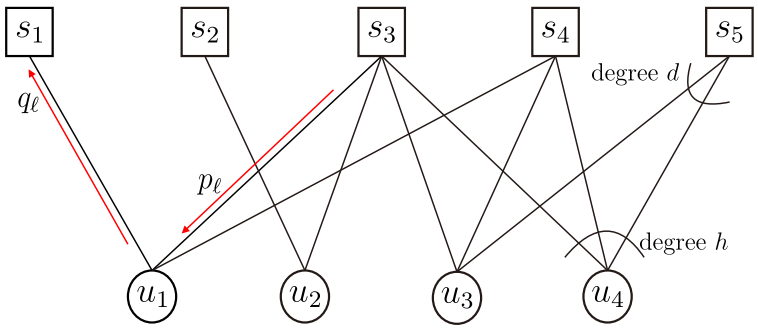

Fig. 4.5: Bipartite graph representation of received signals in one *frame*.

The relay always amplifies and forwards (broadcasts) the received signal to all users. Accordingly, all users receive the same information from the network. We assume that a pointer is equipped in every packets to enable SIC. The pointer contains information on which PTSs the other packets are transmitted. Correspondingly, the connections of users and PTSs can be modeled using a bipartite graph $\mathcal{G} = (\mathcal{U}, \mathcal{S}, \mathcal{E})$ as shown in Fig. 4.5.

The graph $\mathcal{G}$ is composed of set of *user nodes* $\mathcal{U} = \{u_1, u_2, ..., u_{M+1}\}$, set of *slot nodes* $\mathcal{S} = \{s_1, s_2, ..., s_N\}$, and set of edges $\mathcal{E}$ that connect user nodes and slot nodes. The user node represents the user transmitting messages to the networks, while the slot node represents the PTS (slot) chosen by the users to transmit the messages. User node $u_i \in \mathcal{U}$ is connected by an edge $\mathcal{E}_{ij}$ to slot node $s_j \in \mathcal{S}$ if and only if user u_i transmits one of its messages to the network via PTS j. User node u_i has degree h, indicating that the user u_i chooses a code type $c_h \sim (h, k)$ to encode its k data to h packets. On the other hand, slot node s_j has degree d, which expresses that there are d users transmit one of their messages simultaneously to the relay via PTS j. The transmission scheme can also be represented by a matrix with size of $N \times (M + 1)$. For example, matrix

$$A = \begin{bmatrix} 1 & 0 & 0 & 0 \\ 0 & 1 & 0 & 0 \\ 1 & 1 & 1 & 1 \\ 1 & 0 & 1 & 1 \\ 0 & 0 & 1 & 1 \end{bmatrix} \tag{4.4}$$

represents the structure shown in Fig. 4.5. The rows and columns correspond the

PTSs and the users, respectively. The graph and matrix representations described above imply that the proposed uncoordinated transmission scheme resembles a coding structure similar to low-density parity-check (LDPC) codes.

4.3 Proposed Decoding Strategy

Prior to decoding process, each destination subtracts its own messages from the received signals in a *frame*. After subtraction, each user has unique matrix representation with size $N \times M$ as

$$A_1 = \begin{bmatrix} 0 & 0 & 0 \\ 1 & 0 & 0 \\ 1 & 1 & 1 \\ 0 & 1 & 1 \\ 0 & 1 & 1 \end{bmatrix}, A_2 = \begin{bmatrix} 1 & 0 & 0 \\ 0 & 0 & 0 \\ 1 & 1 & 1 \\ 1 & 1 & 1 \\ 0 & 1 & 1 \end{bmatrix}, A_3 = \begin{bmatrix} 1 & 0 & 0 \\ 0 & 1 & 0 \\ 1 & 1 & 1 \\ 1 & 0 & 1 \\ 0 & 0 & 1 \end{bmatrix}, \text{ and } A_4 = \begin{bmatrix} 1 & 0 & 0 \\ 0 & 1 & 0 \\ 1 & 1 & 1 \\ 1 & 0 & 1 \\ 0 & 0 & 1 \end{bmatrix}. \tag{4.5}$$

As example, bipartite graph of user u_1 is is shown in Fig. 4.6 followed by its decoding. With these subtractions, each user experiences different graph-based decoding. However, this difference is negligible when N is large enough.

Decoding is performed iteratively between *network* decoder in user nodes and *physical* decoder in slot nodes. It should be noted here that iterative decoding is performed in the internal receiver, not between the relay and the users. The decoding strategy is illustrated in Fig. 4.6. It is started by finding a slot node with degree $d = 1$, which contains a message from *only* one user (no interference). In this slot node, *physical* decoding is then easily performed using SCC decoder, of which the results are passed to the connected user node. The user node then performs *network* decoding corresponding to the chosen c_h codes. The results of *network* decoding are transferred to the connected slot nodes and used to perform SIC. Accordingly, the degree of the slot nodes are reduced by one. This process is repeated until no slot node with degree $d = 1$ remains, where conventionally, decoding process is stop, resulting low throughput performance.

In this works, we propose a solution by using IDM algorithm to make the decoding does not stop early, but progresses further resulting in larger number of decodable users. With IDM algorithm, the decoding is continued by searching slot nodes with degree $d = 2$, which contains the messages from two users. When

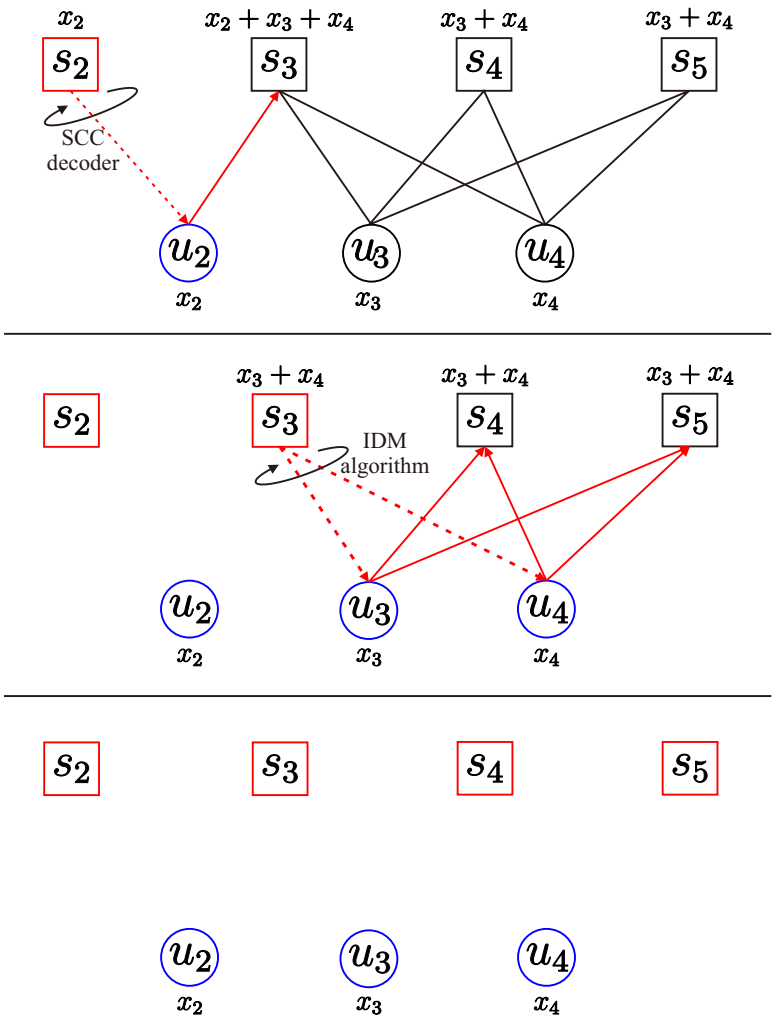

Fig. 4.6: Decoding illustration performed by user u_1 for a system employing irregular repetition codes as the *network* encoder.

degree $d = 2$ is found, the slot node conducts *physical* decoding using IDM algorithm to simultaneously resolve both messages. The results are handed over to the connected user nodes. Similar to the first process, the user nodes perform *network* decoding and transfer the results to the connected slot nodes to be used for interference cancellation. Subsequently, the decoding process is repeated from the first step until no more slot node with degree $d = 1$ or $d = 2$ found or until maximum iteration reached.

4.4 Decoding Convergence Analysis

To answer the quiestion about the maximum achievable performance of MWSRN with IDM algorithm described above, this section provides analysis based on asymptotic assumption. We set number of users and PTSs to be infinite, $\{(M+1), N\} \rightarrow \infty$, while keeping $G = kM/N$ constant. We also assume high received signal-to-noise power ratio (SNR), defined as $\Gamma = P/\sigma^2$, where P is transmit power and σ^2 is noise variance, such that the *physical* decoding exhibits perfect results.

4.4.1 Degree Distributions on Node

In one *frame*, each user selects a type $c_h \sim (h, k)$ code to encode its k data to h packets to be transmitted via h randomly chosen PTSs. The selection of a code is managed according to a probability mass function (*pmf*) $\Lambda = \{\Lambda_1, \Lambda_2, ..., \Lambda_{n_c}\}$, which corresponds to the degree distribution of user nodes. It is convenient to introduce a polynomial to represent the degree distribution of user node from *nodes perspective* as follows

$$\Lambda(x) = \sum_{h=1}^{n_c} \Lambda_h x^h. \tag{4.6}$$

From *edges perspective*, the degree distribution of user nodes is given by

$$\lambda(x) = \frac{\Lambda'(x)}{\Lambda'(1)} \tag{4.7}$$

$$= \sum_{h=1}^{n_c} \lambda_h x^{h-1}, \tag{4.8}$$

where

$$\lambda_h = \frac{\Lambda_h h}{\sum_{h=1}^{n_c} \Lambda_h h} \tag{4.9}$$

is probability of an edge belongs to user node type h.

Number of users transmitting one of their packets simultaneously via PTS j is equivalent to the degree of slot node, d, of which the probability follows binomial distribution

$$\Psi_d = \binom{M}{d} \left(\frac{\overline{h}G}{kM}\right)^d \left(1 - \frac{\overline{h}G}{kM}\right)^{M-d}. \tag{4.10}$$

Introducing the similar polynomial, the degree distribution of slot nodes from *nodes*

perspective is defined as

$$\Psi(x) = \sum_{d \geq 1} \Psi_d x^d. \tag{4.11}$$

If we let $M \to \infty$, we get

$$\Psi(x) = \exp\left(-\frac{\overline{h}}{k} G(1-x)\right) \tag{4.12}$$

$$= \exp\left(-\frac{G}{R_N}(1-x)\right). \tag{4.13}$$

In the similar way of (4.8), the degree distribution of slot nodes from *edges perspective* is defined as

$$\rho(x) = \frac{\Psi'(x)}{\Psi'(1)} = \sum_d \rho_d(x) \tag{4.14}$$

$$= \exp\left(-\frac{G}{R_N}(1-x)\right), \tag{4.15}$$

where ρ_d is probability of an edge belongs to a slot node degree d.

4.4.2 EXIT Functions

As described in the previous section, the proposed MWSRN resembles a coding structure similar to LDPC codes. Consequently, the similar analysis, e.g., density evolution, is applicable for the proposed system.

We evaluate the probability of an edge having unresolved or erasure packet in the forms of p_ℓ and q_ℓ. As shown in Fig. 4.5, p_ℓ and q_ℓ are the probabilities of an edge emanating from slot node to user node and user node to slot node, respectively, carrying an erasure at iteration ℓ.

Let consider a user node type h as a user node that chooses *network* encoder c_h. Similar to [9], the probability of an edge carrying erasure coming out from the user node type h at iteration ℓ is defined as

$$q_\ell^{(h)} = \frac{1}{h} \sum_{t=0}^{h-1} p_{\ell-1}^t (1-p_{\ell-1})^{h-1-t} \left[(h-t)\tilde{e}_{h-t}^{(h)} - (t+1)\tilde{e}_{h-1-t}^{(h)}\right] := f_u^{(h)}(p_{\ell-1}), \tag{4.16}$$

where $\tilde{e}_g^{(h)}$ is g-th un-normalized information function for the code $c_h \in \mathcal{C}$ [22] and $f_u^{(h)}(p_{\ell-1})$ is extrinsic information transfer (EXIT) function for a user node type

$$1 - p_\ell = (1 - q_\ell)^{d-1} \qquad 1 - p_\ell = (d-1)q_\ell(1 - q_\ell)^{d-2}$$

(a) (b)

Fig. 4.7: The probability of an edge is not carrying erasure packet outgoing from a slot node degree d (a) without and (b) with IDM algorithm.

h [23].

Averaging over the edges, we obtain the EXIT function for user nodes, which is defined as the probability of an edge outgoing from user nodes carrying erasure

$$q_\ell = f_u(p_{\ell-1}) \tag{4.17}$$

$$= \sum_{h=1}^{n_c} \lambda_h f_u^{(h)}(p_{\ell-1}). \tag{4.18}$$

Incorporating (4.16) into (4.18), we derive

$$f_u(p_{\ell-1}) = \sum_{h=1}^{n_c} \frac{\lambda_h}{h} \sum_{t=0}^{h-1} p_{\ell-1}^t (1 - p_{\ell-1})^{h-1-t} \left[(h-t)\tilde{e}_{h-t}^{(h)} - (t+1)\tilde{e}_{h-1-t}^{(h)} \right] \tag{4.19}$$

$$= \frac{1}{\overline{h}} \sum_{h=1}^{n_c} \Lambda_h \sum_{t=0}^{h-1} p_{\ell-1}^t (1 - p_{\ell-1})^{h-1-t} \left[(h-t)\tilde{e}_{h-t}^{(h)} - (t+1)\tilde{e}_{h-1-t}^{(h)} \right]. \tag{4.20}$$

Using insights from [10], EXIT function of slot nodes is derived. In the proposed decoding strategy with IDM algorithm, a degree d slot node can be perfectly decoded if number of incoming edges carrying erasures is less than or equal to *two*, which corresponds to the IDM algorithm capability of decoding *two* messages

simultaneously. As illustrated in Fig. 4.7, this probability is given by

$$1 - p_\ell = (1 - q_\ell)^{d-1} + (d-1)q_\ell(1 - q_\ell)^{d-2}. \tag{4.21}$$

By averaging over the edges, we obtain

$$p_\ell = \sum_d \rho_d \left[1 - (1 - q_\ell)^{d-1} - (d-1)q_\ell(1 - q_\ell)^{d-2}\right], \tag{4.22}$$

which is further expanded to

$$p_\ell = \sum_d \rho_d - \sum_d \rho_d (1 - q_\ell)^{d-1} - \sum_d \rho_d (d-1) q_\ell (1 - q_\ell)^{d-2}, \tag{4.23}$$

$$= 1 - \rho(1 - q_\ell) - q_\ell \rho'(1 - q_\ell), \tag{4.24}$$

where $\rho(\cdot)$ is defined in (4.15), from which we can also get

$$\rho'(x) = \frac{G}{R_N} \exp\left(-\frac{G}{R_N}(1 - x)\right). \tag{4.25}$$

Therefore, (4.24) becomes

$$p_\ell = 1 - \left(1 + q_\ell \frac{G}{R_N}\right) e^{-q_\ell \frac{G}{R_N}} := f_s(q_\ell), \tag{4.26}$$

that defines the EXIT function of slot nodes, $f_s(q_\ell)$.

The well-known EXIT chart is used to visualize the evolution of erasure functions from the both nodes. As an example, we analyze the proposed MWSRN employing irregular repetition codes as *network* encoder. In this case, EXIT function of user node defined in (4.20) can be simplified to

$$f_u(p_{\ell-1}) = \sum_{h=2}^{n_c} \lambda_h p_{\ell-1}^{h-1}, \tag{4.27}$$

while EXIT function of slot node remains the same. It is important to note here that $h = 1$ should be avoided to ensure the decoding stability.

In Fig. 4.8, EXIT chart of MWSRN employing irregular repetition codes with degree distribution $\Lambda_{\mathrm{a}}(x) = 0.5x^2 + 0.28x^3 + 0.22x^8$, rate $R_N = 0.278$, and offered

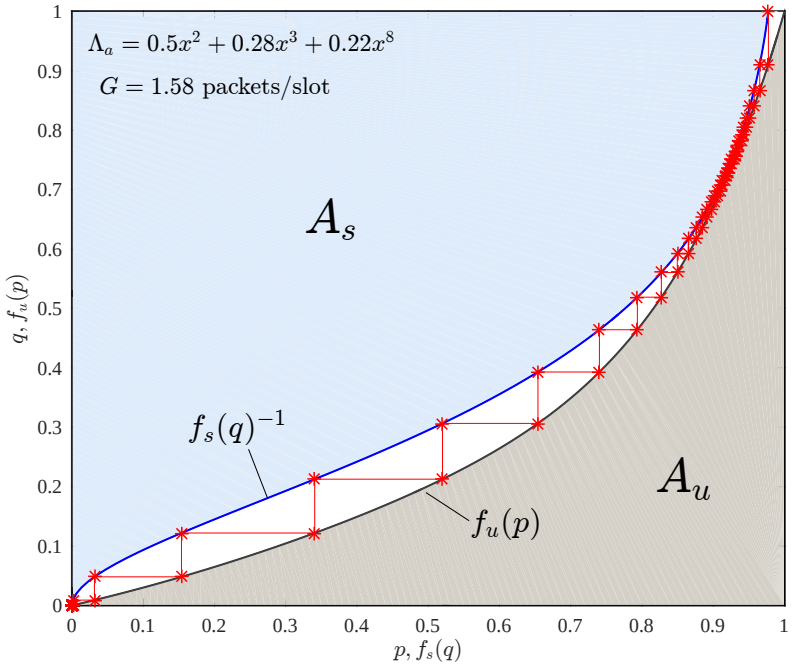

Fig. 4.8: EXIT Chart with successful decoding for MWSRN with irregular repetition code and user nodes degree distribution $\Lambda_a(x) = 0.5x^2 + 0.28x^3 + 0.22x^8$, rate $R_N = 0.278$, and offered traffic $G = 1.58$ packets/slot.

traffic $G = 1.58$ packets/slot[1] is presented. The evolution of probability of an edge carrying erasure from user node (q_ℓ) and slot node (p_ℓ) converges to zero in a sufficient iteration if and only if there is an open tunnel between two EXIT curves $f_u(p)$ and $f_s(q)^{-1}$ (no intersection between two EXIT curves). This condition is satisfied when the offered traffic is set below the threshold, G^*, which is defined as the maximum value of G such that the EXIT curves $f_u(p)$ and $f_s(q)^{-1}$ do not intersect each other. For $\Lambda_a(x)$ we obtain that G^* equal to 1.59 packets/slot.

Contrarily, when $G > G^*$, the pair of probabilities (p_ℓ, q_ℓ) will never converge to $(0, 0)$ even with infinite iterations. This condition is exemplified in Fig. 4.9, where EXIT chart of MWSRN employing $\Lambda_a(x)$ with $G = 1.60 > G^*$ is drawn. The trajectory of the EXIT chart is stuck in non-$(0, 0)$ point, implying an early decoding failure.

In Table 4.1, we present the average network rate R_N and threshold G^* of MWSRN with several degree distributions of irregular repetition codes. This table

[1]Please note that in this chapter, the term *slot* is corresponding to *PTS*.

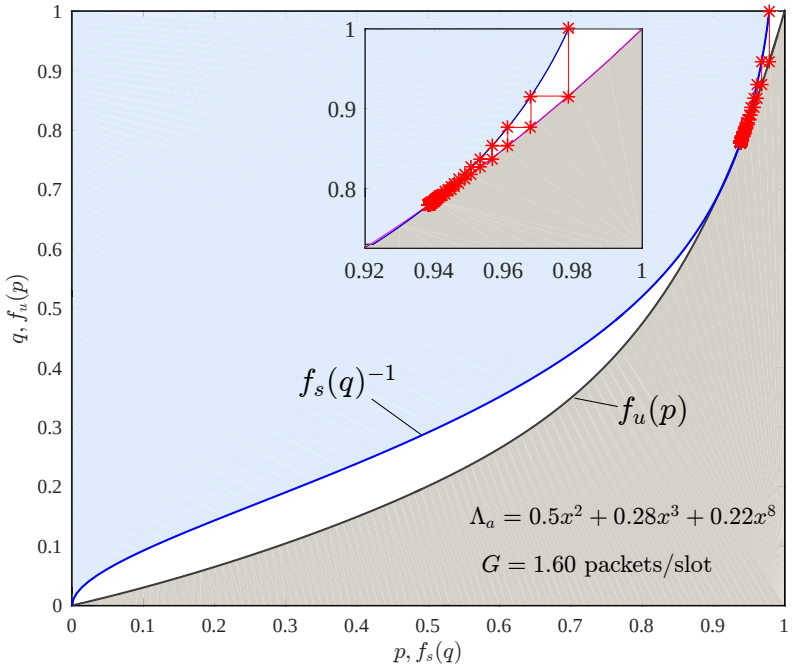

Fig. 4.9: EXIT Chart with failure decoding for a MWSRN with irregular repetition code and user nodes degree distribution $\Lambda_{\mathrm{a}}(x) = 0.5x^2 + 0.28x^3 + 0.22x^8$, rate $R_N = 0.278$, and offered traffic $G = 1.60$ packets/slot.

Table 4.1: Thresholds of Offered Traffic Load (G^*) for Various User Nodes Degree Distributions.

Id	**Degree Distributions**	R_N	G^*
$\Lambda_{\mathrm{a}}(x)$	$0.5x^2 + 0.28x^3 + 0.22x^8$	0.2778	1.59
$\Lambda_{\mathrm{b}}(x)$	$0.25x^2 + 0.60x^3 + 0.15x^8$	0.2857	1.56
$\Lambda_{\mathrm{c}}(x)$	$0.5465x^2 + 0.1623x^3 + 0.2912x^6$	0.3006	1.61
$\Lambda_{\mathrm{d}}(x)$	$0.2x^2 + 0.2x^3 + 0.2x^4 + 0.2x^5 + 0.2x^6$	0.2500	1.38
$\Lambda_{\mathrm{e}}(x)$	$0.5102x^2 + 0.4898x^4$	0.3356	1.62

also indicates that the user nodes degree distribution is a parameter subject to optimization in terms of R_N or G^*.

4.4.3 Network Capacity Bound

Area theorem of EXIT chart is utilized to derive *network* capacity bound of MWSRN. Please note that network capacity bound in this thesis is defined as

the bound indicating maximum traffic (G^*) that can be achieved by the proposed MWSRN. The necessary condition of successful decoding is the existence of an open tunnel between two EXIT curves. In other words, the sum of the area under the curve $f_u(p)$, denoted as A_u, and area under the curve $f_s(q)$, denoted as A_s, is less than 1 (see Fig. 4.8). This condition can be written as

$$A_s + A_u < 1, \tag{4.28}$$

where

$$A_s = \int_0^1 f_s(q)\mathrm{d}q \tag{4.29}$$

and

$$A_u = \int_0^1 f_u(p)\mathrm{d}p. \tag{4.30}$$

From (4.28) - (4.30) we obtain

$$R_N + \left(1 + \frac{2R_N}{G}\right) e^{-G/R_N} - \frac{2R_N}{G} < 0, \tag{4.31}$$

which is the network capacity bound of the proposed MWSRN employing IDM algorithm. Although (4.31) is not in the closed-form, with some mathematical manipulations, it is easy to find its positive solutions, i.e., $G \geq 0$ and $R_N \geq 0$. These solutions are drawn in Fig. 4.10 and compared to the MWSRN employing conventional CSA without IDM algorithm. The maximum threshold G^* of 2 packets/slot can be achieved theoretically by the proposed MWSRN using very low R_N. The threshold R_N and G^* of the MWSRN with degree distributions presented in Table 4.1 are also shown in Fig. 4.10 to confirm the achievable points under the bound. The bound indeed can be approached by optimizing the degree distribution of the user nodes [24].

4.5 Performances Evaluations

In this section we evaluate the performances of the proposed MWSRN using series of computer simulations. For the sake of simplicity, we conduct simulation for MWSRN with irregular repetition codes as the *network* encoder. In the *physical* encoder, we utilize SCC codes, where half rate memory-1 convolutional code $[3, 2]_8$

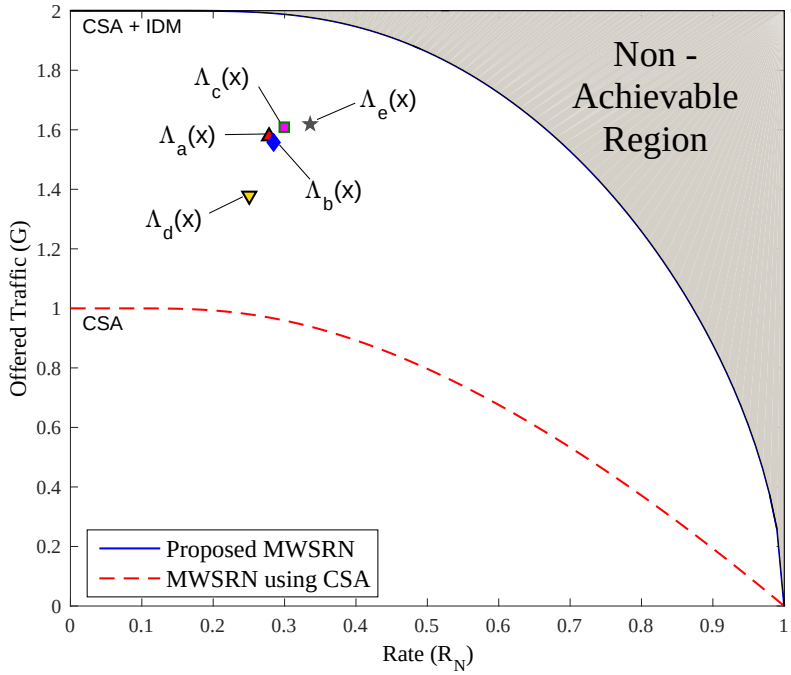

Fig. 4.10: The network capacity bound of the proposed MWSRN compared to the MWSRN employing conventional CSA.

is serially concatenated with doped accumulator (ACC). The total rate of the physical encoder is $R_P = 0.5$.

The simulation is carried out over additive white Gaussian noise (AWGN) channel. The channels between users and relay in MAC and BC phases are equal to 1. Each user uses an equal power $P_i = P$ to transmit its message to relay. The variance of AWGN in all users and the relay are also assumed to be equal, $\sigma_i^2 = \sigma_r^2 = 1$. The relay amplification factor of $B = 2$ is considered.

We first investigate packet-loss-rate (PLR) and throughput performances of the proposed system. For this, high SNR is assumed such that the *physical* decoder can decode the messages perfectly. The comparison is made between the proposed MWSRN and the MWSRN using conventional irregular repetition slotted ALOHA (IRSA) [8], which is regarded as the special case of CSA with a repetition codes $(h, 1)$. The number of PTSs is fixed to $N = 200$ (because in practice N can not be set too long) and number of users M is varying according to value of the offered traffic G. We employ user nodes degree distributions $\Lambda_{\mathrm{a}}(x)$ and $\Lambda_{\mathrm{b}}(x)$. The results in terms of PLR are plotted in Fig. 4.11 accompanied by the asymptotic

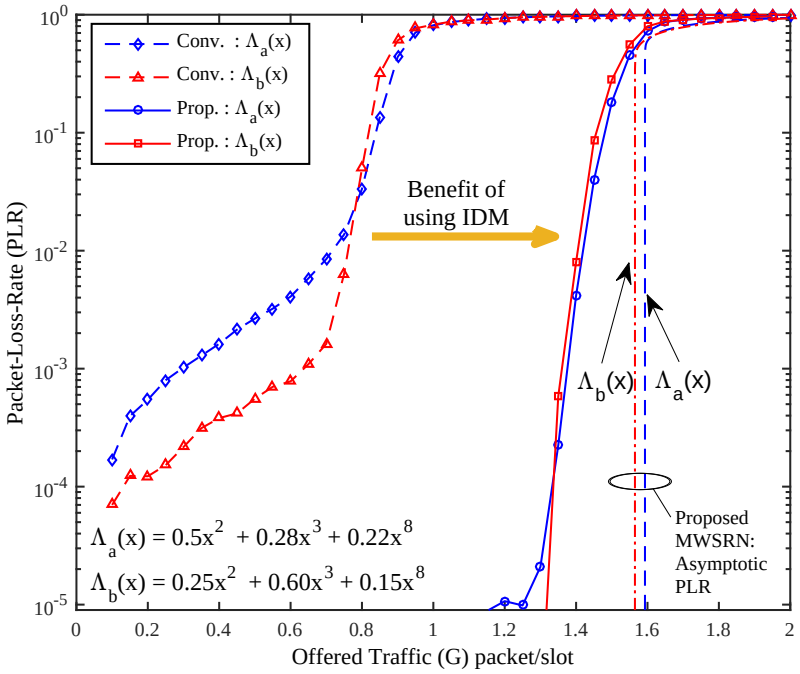

Fig. 4.11: Packet-loss-rate (PLR) performances of MWSRN with the proposed technique and conventional IRSA employing $\Lambda_{\mathrm{a}}(x)$ and $\Lambda_{\mathrm{b}}(x)$.

PLR obtained from EXIT chart analysis.

Fig. 4.11 shows the superiority of the proposed MWSRN compared to MWSRN employing conventional technique without IDM algorithm (IRSA). In achieving a certain level of PLR, the proposed MWSRN offers higher traffic. For instance, with $\Lambda_{\mathrm{a}}(x)$, the proposed MWSRN can achieve PLR of 10^{-3} with offered traffic close to 1.4 packets/slot, while the conventional MWSRN achieves it with smaller traffic $G = 0.25$ packets/slot. Furthermore, the proposed MWSRN offers very low PLR floor, which is less than 10^{-5} for $\Lambda_{\mathrm{a}}(x)$ and $\Lambda_{\mathrm{b}}(x)$. Fig. 4.11 also shows the asymptotic limit of PLR, where PLR cliff occurs around $G = 1.6$ packets/slot. This asymptotic limit value can be further increased by choosing an optimal degree distribution of user nodes. The results presented in this figure confirm that the proposed system is working very well even with $G \geq 1$ packet/slot.

Since the proposed MWSRN exhibits PLR floor, throughput analysis is of significant importance. Fig. 4.12 shows the final throughput performances obtained from the PLR. It is confirmed that the throughput of the proposed MWSRN is more excellent compared to the conventional MWSRN employing IRSA and slotted

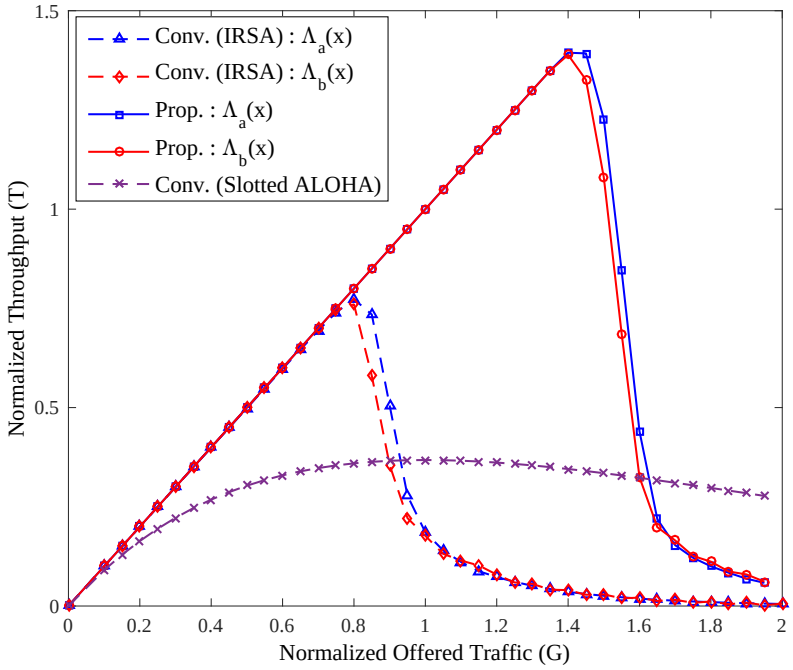

Fig. 4.12: Throughput performances of MWSRN.

ALOHA. The maximum throughput achieved by the well-known slotted ALOHA is 0.367 packets/slot, while for the IRSA with $\Lambda_{\rm a}(x)$ and $\Lambda_{\rm b}(x)$ are around 0.76 packets/slot. Exceptionally, the proposed MWSRN achieves maximum throughput of around 1.4 packets/slot, which is beyond 1 packets/slot.

In Fig. 4.13, bit-error-rate (BER) performances of the proposed MWSRN with $M = 101$ users, $N = 90$ PTSs, and varrying values of SNR are presented. Correspondingly, the value of G is equal to 1.11 packets/slot. The degree distributions of user nodes employed in the systems are $\Lambda_{\rm a}(x)$, $\Lambda_{\rm b}(x)$, and $\Lambda_{\rm c}(x)$. It is shown that a reliable communication with BER lower than 10^{-5} can be achieved with $P > 3.2$ dB. We also observe that turbo cliffs of BER performances similar to that of [11] occur in the proposed MWSRN. These results also indicate that the proposed system can work properly in a relatively low SNR environment.

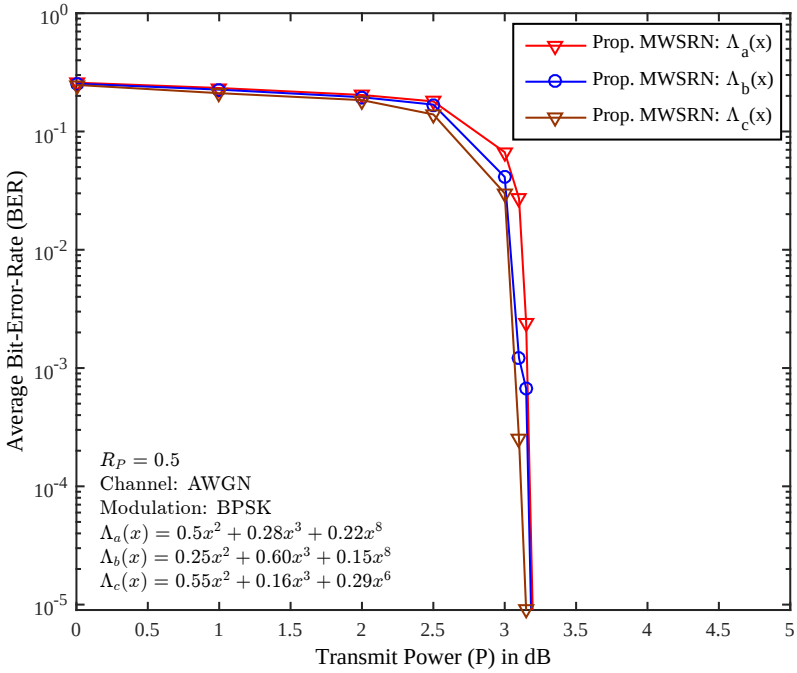

Fig. 4.13: BER performances of the proposed MWSRN with $\Lambda_{\mathrm{a}}(x)$, $\Lambda_{\mathrm{b}}(x)$, and $\Lambda_{\mathrm{c}}(x)$.

4.6 Summary

This chapter aims to introduce uncoordinated transmission scheme for MWSRN and propose a novel decoding strategy that can significantly enhance the throughput performance.

We first described the system model of MWSRN and analyzed the proposed uncoordinated transmission strategy that is very favorable for networks with *massive* number of users. We showed that the proposed MWSRN resembles the coding structure similar to LDPC codes that can be represented by a bipartite graph. Thus, *graph-based* decoding strategy in the form of SIC is exploited to effectively decode all messages transmitted in uncoordinated fashion.

We then proposed IDM algorithm to be incorporated into *graph-based* SIC to break the limit of throughput $T = 1$ packet/slot. EXIT chart was used to analyze the decoding convergence behavior of the proposed techniques. We derived the evolution functions of probability of an edge carrying erasure messages during iterative decoding process and plot them into EXIT chart to visualize the decoding convergence. Subsequently, we exploited EXIT chart area theorem to derive the

network capacity bound of the proposed MWSRN, which is almost two times higher compared to the conventional MWSRN employing CSA.

The results of performances evaluations was also presented in this chapter. It was shown that the proposed MWSRN with IDM algorithm outperforms the conventional MWSRN without IDM algorithm in terms of PLR and throughput performances. The results also showed that the proposed MWSRN can reliably operate in a relatively low SNR environment.

Chapter 5

Multiway Multirelay Networks

In this chapter, we extend the results obtained in the previous chapter to the cases where multiple relays are considered in MWRN, called *multiway multirelay networks* (MWMRN). We consider two scenarios: (i) MWMRN serving users in two clusters with two relays, termed as MWMRN-2C, and (ii) MWMRN serving randomly distributed users in an area supported by arbitrary number of relays, termed as D-MWMRN. In both scenarios, we adopt *modern* decode-and-forward (mDF) protocol [12], where the relays keep broadcasting the messages even though the received messages are erroneous. Final joint decoding is proposed to improve networks performances by exploiting source correlations of the messages.

In the first scenario, we employ uncoordinated transmission in MAC phase. However, to verify the contribution of multiple relays, IDM is not incorporated into SIC. Rather, we focus on the proposed final joint decoding and show its superiority performances. We also confirm the acuracy of the estimation of messages correlation that is exploited in the final joint decoding to improve the networks performances.

We then proceed to more general cases in the second scenario, where arbitrary number of relays are considered to serve *massive* number of users randomly distributed in an area. We generalize the proposed final joint decoding for arbitrary number of relays and investigate the practical optimal number of relays.

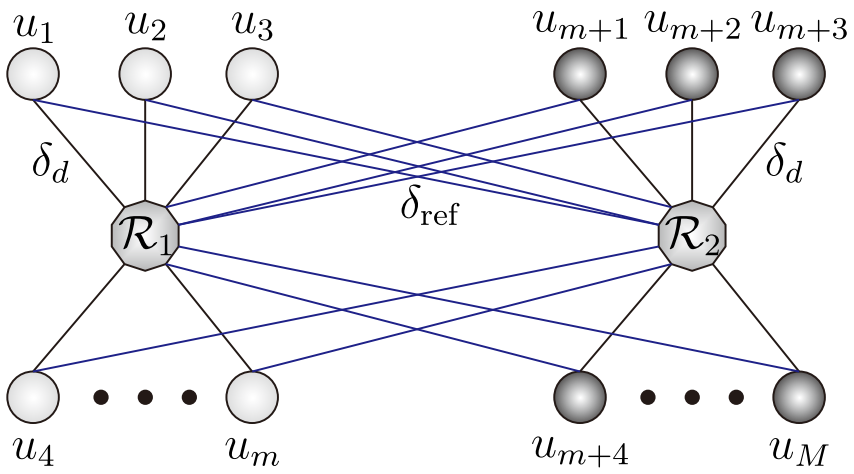

Fig. 5.1: System model of MWMRN-2C: two clusters of users and two relays, $\mathcal{R}_1$ and $\mathcal{R}_2$.

5.1 Multiway Multirelay Networks with Two Clusters

5.1.1 System Model

System model of MWMRN-2C is described in Fig. 5.1, where M users are divided into two groups (clusters) based on their distances to the nearest relay. All users exchange information among themselves with the help of two relays, $\mathcal{R}_1$ and $\mathcal{R}_2$. Each user has distance δ_d to the nearest relay and δ_{ref} to another relay. All users have equal transmit power P_u, and similarly both relays also have equal transmit power $P_{\mathcal{R}}$. In MAC phase, SNR from users to the relay with distance δ_{ref} is $\Gamma_{u,\mathcal{R},\text{ref}} = P_{\mathcal{R}}/\sigma^2$, where σ^2 is noise variance. While SNR from users to the relay with distance δ_d is $\Gamma_{u,\mathcal{R},d} = \Gamma_{u,\mathcal{R},\text{ref}}(\delta_d/\delta_{\text{ref}})^\gamma$, and γ is a pathloss exponent. We assume $\gamma = 3.52$ [12]. In BC phase, SNR from relay to the users with distance δ_{ref} is $\Gamma_{\mathcal{R},u,\text{ref}} = P_{\mathcal{R}}/\sigma^2$, while SNR from relay to the users with distance δ_d is $\Gamma_{\mathcal{R},u,d} = \Gamma_{\mathcal{R},u,\text{ref}}(\delta_d/\delta_{\text{ref}})^\gamma$.

We assume half-duplex mode in the transmission scheme with perfect frame and slot synchronizations. All users perform information exchange within one *frame* composed of $L = (N + 2M)$ time slots (TS).[1] Each TS has equal time duration T_s. The first N of L TSs are utilized in MAC phase, while the remaining $2M$ TSs are used in BC phase.

[1]Note that in this chapter, instead of *PTS*, we use *TS* since mDF protocol is adopted in the relays.

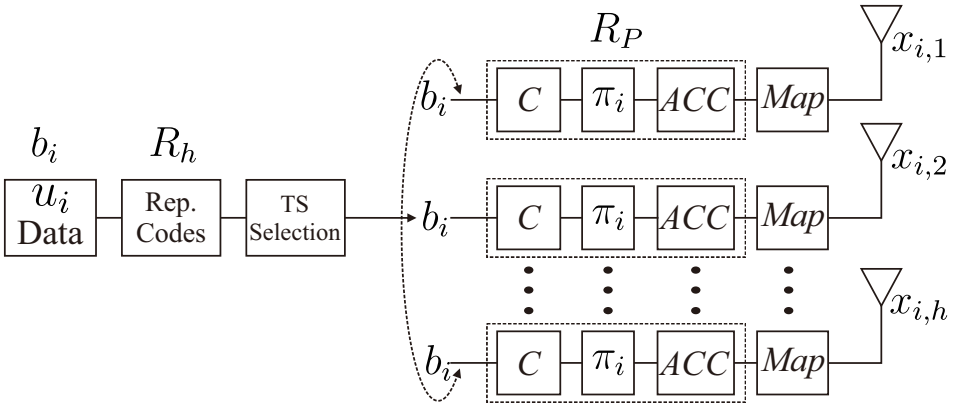

Fig. 5.2: Transmitter structure of user u_i with two encoders: network encoder R_h and physical encoder R_P.

In MWMRN-2C, we define *logical* offered traffic load, G, as number of messages to be sent divided by number of TSs used to deliver the messages. Assuming that each user has one message, the offered traffic from networks to *one user* is defined as

$$G_{\mathrm{U}} = \frac{M-1}{L} = \frac{M-1}{N+2M}. \tag{5.1}$$

For the BC phase, since the relays requires $2M$ TSs in total to transmit all the messages of M users, the offered traffic addressed to *every user* is

$$G_{\mathrm{BC}} = \frac{M-1}{2M}. \tag{5.2}$$

Unlike BC phase, MAC phase is more dynamic with the uncoordinated transmission schemes. Number of TSs N can be further optimized to maximize the throughput of the systems. The offered traffic in the MAC phase is given by

$$G_{\mathrm{MAC}} = \frac{M}{N}. \tag{5.3}$$

5.1.2 Multiple Access Channel (MAC) Phase

5.1.2.1 Transmission Strategy in MAC Phase

Transmitter structure of user u_i, as illustrated in Fig. 5.2, utilizes two encoders: *network* encoder to combat error or interference caused by *uncoordinated* transmission, and *physical* encoder that acts as channel encoder.

Set of *packet-oriented* repetition codes, $\mathcal{C} = \{c_h\}_{h=2}^{n_c}$, are available in the systems to be randomly picked by each user as *network* encoder. For $h \in \{2, 3, ..., n_c\}$, code $c_h \sim (h, 1)$ has length h, dimension 1, and rate $R_h = 1/h$.[2] User u_i encodes its data, b_i, using c_h chosen randomly from set $\mathcal{C}$ according to probability mass function (*pmf*) $\Lambda = \{\Lambda_h\}_{h=2}^{n_c}$, where $\sum_{h=2}^{n_c} \Lambda_h = 1$. We then define *average network rate* as $R_N = 1/\overline{h}$, where $\overline{h} = \sum_{h=2}^{n_c} \Lambda_h h$ is the expected length of the codes.

Network encoder produces h packets of b_i, and therefore the user requires h TSs to transmit them. The h TSs are chosen uniformly random from set of TSs $\mathcal{S} = \{s_1, s_2, ..., s_N\}$, which are the first N TSs of the transmission *frame*. The packets are then further encoded using *physical* encoder using SCC composed of convolutional codes C, random interleaver π_i, and doped-accumulator ACC. Total rate of *physical* encoder is R_P. The outputs of ACC are modulated by *Map*, producing x_i. We assume x_i is BPSK symbols having $E[|x_i|^2] = 1$. Prior to transmission via the selected TSs, the packets are equipped with a pointer containing information about location of other packets. The pointer is exploited for SIC in the decoding process.

After N TSs, relay $\mathcal{R}_r$, $r \in \{1, 2\}$, receives

$$Y_r = AX_r + Z_r, \tag{5.4}$$

with

$$Y_r = [y_{r,1}\ y_{r,2}\ ...\ y_{r,N}]^T, \tag{5.5}$$

$$X_r = [\sqrt{\Gamma_{u_1,\mathcal{R}_r}}x_1\ \sqrt{\Gamma_{u_2,\mathcal{R}_r}}x_2\ ...\ \sqrt{\Gamma_{u_M,\mathcal{R}_r}}x_M]^T, \tag{5.6}$$

$$Z_r = [z_{r(1)}\ z_{r(2)}\ ...\ z_{r(N)}]^T, \tag{5.7}$$

$$A = \begin{bmatrix} a_{1,1} & a_{1,2} & ... & a_{1,M} \\ a_{2,1} & a_{2,2} & ... & a_{2,M} \\ ... & .... & a_{j,i} & ... \\ a_{N,1} & a_{N,2} & ... & a_{N,M} \end{bmatrix}, \tag{5.8}$$

where $y_{r,j}$ is the received signal at relay $\mathcal{R}_r$ at TS s_j, z_r is AWGN noise at relay $\mathcal{R}_r$ with variance $\sigma_r^2 = 1$, and $a_{j,i}$ takes value 1 if TS s_j is selected by user u_i, and takes 0 otherwise.

[2]Please note that we do not use repetition code with degree 1, $c_1 \sim (1, 1)$, since it causes the systems unstable.

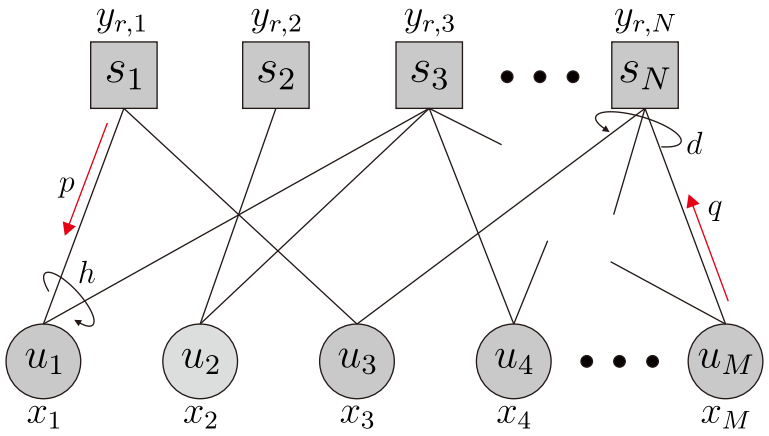

Fig. 5.3: Bipartite graph representing uncoordinated transmission strategy from all users to relay $\mathcal{R}_r$ in MAC phase.

5.1.2.2 Decoding Strategy in Relays

In MAC phase, the uncoordinated transmission scheme expressed by matrix A in (5.8), can also be represented by a bipartite graph $\mathcal{G} = (\mathcal{U}, \mathcal{S}, \mathcal{E})$ as shown in Fig. 5.3. The graph is comprised of set of *user nodes* $\mathcal{U} = \{u_1, u_2, ..., u_M\}$ representing users, set of *slot nodes* $\mathcal{S} = \{s_1, s_2, ..., s_N\}$ representing TSs, and set of edges $\mathcal{E}$ connecting the user nodes and slot nodes.[3] An edge $e_{j,i}$ connects user node u_i to slot node s_j if and only if $a_{j,i} = 1$.

As shown in Fig. 5.3, user nodes have degree h and slot nodes have degree d. Degree h of user node u_i means that user u_i picks code c_h, and thus transmits its information h times. On the other hand, degree d of slot node s_j means that there are d users that select TS s_j to transmit their messages simultaneously to the relays.

Decoding is performed iteratively between *network* decoding in user nodes and *physical* decoding in slot nodes.[4] The *network* decoding corresponds to the decoding of repetition code, while *physical* decoding corresponds to the decoding of SCC codes.

Decoding in the relays is started by finding degree $d = 1$ slot node. *Network* decoding is performed in the slot node the results of which are passed to the connected user node to be used for *physical* decoding. The user node then transfers its

[3] We use the same notation for user nodes (slot nodes) and user (TS) since they are corresponding to each other.

[4] The decoding is performed iteratively inside the relays.

results to the connected slot nodes. Subsequently, SIC is performed by subtracting the decoded messages from the composite signals in the connected slot nodes.

The aforementioned processes are repeated until no more slot node with degree $d = 1$ found or until maximum iteration is reached. Please note that IDM algorithm is not incorporated into SIC in this section, and therefore, the decoding processes stop when no more slot node with degree $d = 1$ found.

5.1.2.3 Decoding Analysis in Relays

EXIT analysis is used to observe the decoding convergence in the asymptotic setting. We assume that SNR is high enough, and $\{M,\ N\} \rightarrow \infty$, while $G_{\text{MAC}} = M/N$ is constant.[5] Since irregular repetition codes is employed as *network* encoder and IDM algorithm is not incorporated into SIC, the asymptotic analysis in this networks is almost similar to that of IRSA [8].

We first define degree distributions of both nodes. From nodes perspective, degree distribution of user nodes follows the *pmf* of *network* encoder selection, Λ, as

$$\Lambda(x) = \sum_{h=2}^{n_c} \Lambda_h x^h, \tag{5.9}$$

while from edges perspective, it is defined as

$$\lambda(x) = \frac{\Lambda'(x)}{\Lambda'(1)} = \sum_{h=2}^{n_c} \lambda_h x^{h-1}, \tag{5.10}$$

where

$$\lambda_h = \frac{\Lambda_h h}{\sum_{h=2}^{n_c} \Lambda_h h} = \frac{\Lambda_h h}{\overline{h}}. \tag{5.11}$$

For slot nodes, the degree distribution follows Poisson distribution due to the fact that TSs are selected randomly with uniform distribution. The degree distribution from nodes and edges perspectives are the same, which are given by

$$\Psi(x) = \sum_{d} \Psi_d x^d = \exp\left(-\frac{G_{\text{MAC}}}{R_N}(1-x)\right), \tag{5.12}$$

$$\rho(x) = \sum_{d} \rho_d x^{d-1} = \exp\left(-\frac{G_{\text{MAC}}}{R_N}(1-x)\right), \tag{5.13}$$

[5]Please note that high SNR is assumed only for asymptotic analysis. This chapter evaluates MWMRN with finite TS and finite SNR.

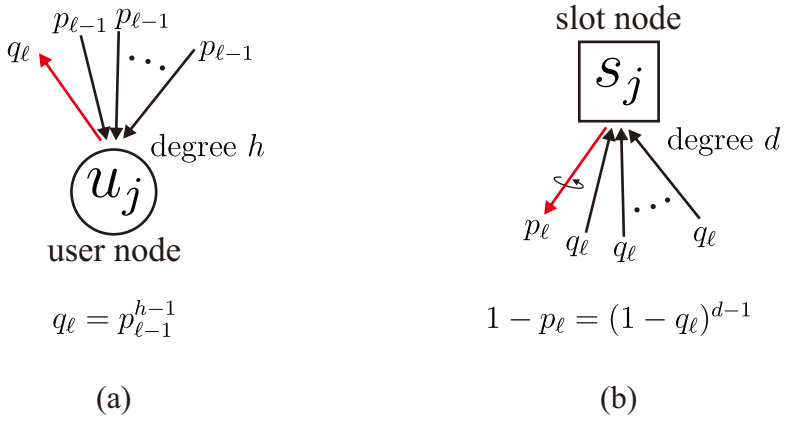

Fig. 5.4: The probability of an edge carrying erasure messages from (a) user node and (b) slot nodes.

respectively.

The decoding convergence can be evaluated by observing evolution of probability of an edge carrying *unresolved* or erasure messages from user nodes to slot nodes and vice versa by iteration. We denote probabilities of an edges carrying erasure messages from *user nodes to slot nodes* and from *slot nodes to user nodes* at iteration ℓ as q_ℓ and p_ℓ, respectively. As illustrated in Fig. 5.4(a), in a user node with degree h, the outgoing edge is carrying erasure messages if all the $h-1$ incoming edges are carrying erasure messages, and hence,

$$q_\ell^{(h)} = p_{\ell-1}^{h-1}. \tag{5.14}$$

However, for slot nodes as shown in Fig. 5.4(b), the outgoing edge of slot node with degree d is *not* containing erasure messages if all the $d-1$ incoming edges are *not* containing erasure messages. In other words, we can express it as

$$p_\ell^{(d)} = 1 - (1 - q_\ell)^{d-1}. \tag{5.15}$$

By averaging over the edges, we obtain

$$q_\ell = \sum_{h=2}^{n_c} \lambda_h p_{\ell-1}^{h-1} := f_u(p_{\ell-1}), \tag{5.16}$$

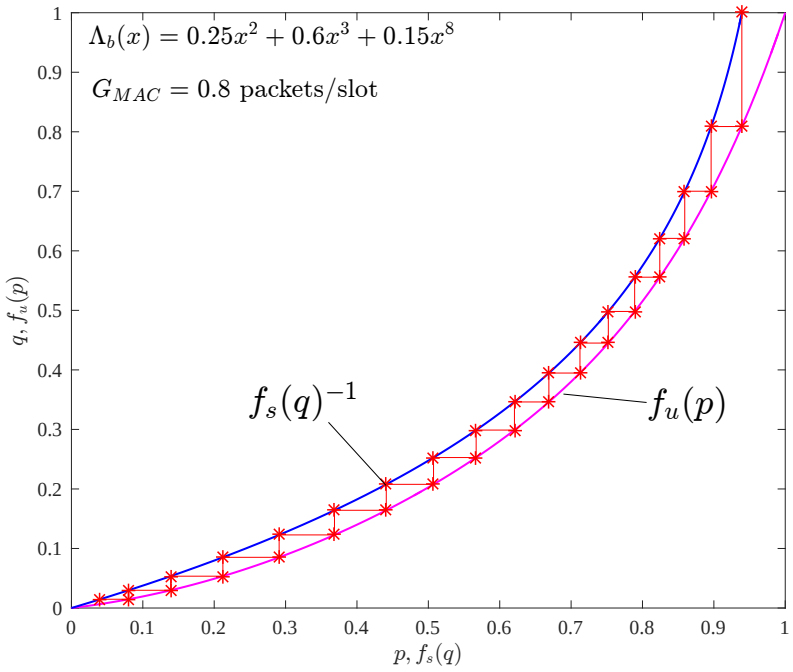

Fig. 5.5: EXIT chart of uncoordinated transmission in MAC phase using irregular repetition codes with degree distribution $\Lambda_{\mathrm{b}}(x) = 0.25x^2 + 0.6x^3 + 0.15x^8$ with $G_{\mathrm{MAC}} = 0.8$ packets/slot.

$$p_\ell = 1 - e^{-q_\ell \frac{G_{\mathrm{MAC}}}{R_N}} := f_s(q_\ell), \tag{5.17}$$

where f_u is EXIT function of user nodes and f_s is EXIT function of slot nodes.

EXIT chart is used to visualize the decoding convergence behavior using EXIT functions derived in (5.16) and (5.17). We provide an example of EXIT chart for networks having user nodes degree distribution $\Lambda_{\mathrm{b}}(x) = 0.25x^2 + 0.6x^3 + 0.15x^8$ and $G_{\mathrm{MAC}} = 0.8$ packets/slot in Fig. 5.5.[6] The evolution of (q, p) are visualized by the trajectory, which is also indicating the required iterations given the open tunnel. The decoding is successful with high probability if the trajectory progresses until point $(0, 0)$ indicating that no erasure in the networks (all nodes are resolves). This condition is characterized by the existence of *open tunnel* between two curves in the EXIT chart. In other words, two curves do not intersect each other, yielding $(q_\ell, p_\ell) \to (0, 0)$ when $\ell \to \infty$. It should be noted here that narrower tunnel requires higher number of iterations, which is also implying the higher efficiency

[6]The *slot* in this chapter is corresponding to *times slot* (TS).

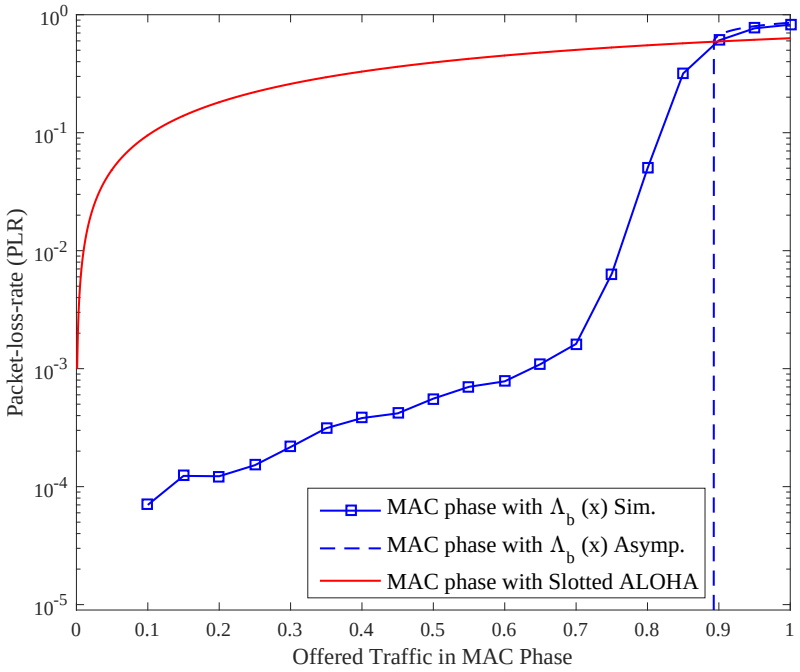

Fig. 5.6: PLR performances of uncoordinated transmission in MAC phase with degree distribution $\Lambda_{\rm b}(x) = 0.25x^2 + 0.6x^3 + 0.15x^8$.

of the networks.

The threshold of offered traffic $G^*_{\rm MAC}$ is defined as the maximum value of $G_{\rm MAC}$ such that the successful decoding condition is satisfied. The $G^*_{\rm MAC}$ also corresponds to the maximum throughput in MAC phase to be achieved asymptotically by networks given the user nodes degree distribution. For $\Lambda_{\rm b}(x)$, the $G^*_{\rm MAC}$ is 0.891 packets/slot.

5.1.2.4 Evaluations of MAC Phase Performances

We evaluate PLR and throughput performances of MAC phase by assuming high enough SNR. Fig 5.6 shows PLR performances of the proposed networks with $\Lambda_{\rm b}(x)$ and the well-known slotted ALOHA (SA). It can clearly be seen that the proposed networks yields lower PLR compared to the networks with SA. With $G_{\rm MAC} = 0.5$ packets/slot, the proposed networks offers PLR of around 10^{-3}. In terms of throughput performance, the proposed networks also provides significant improvement compared to the networks employing SA, as shown in Fig. 5.7. It

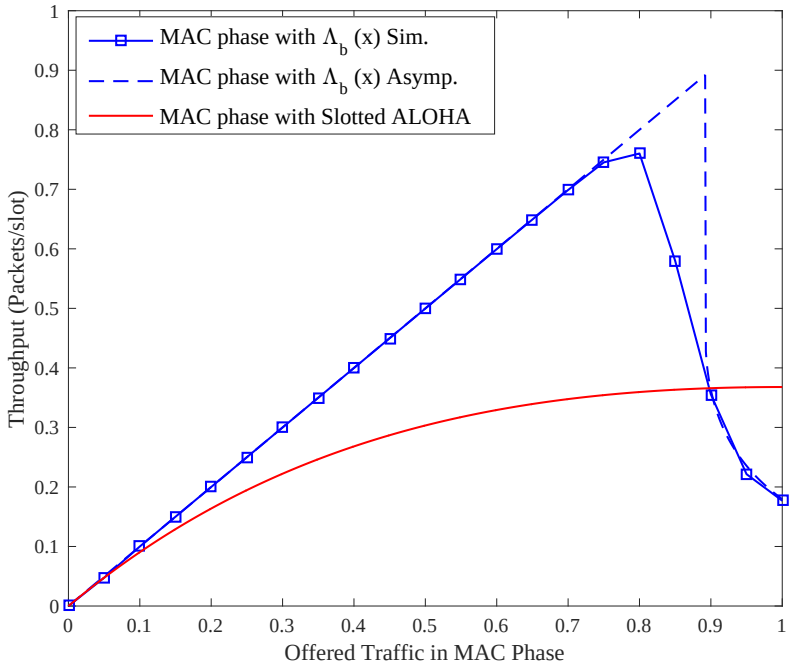

Fig. 5.7: Throughput performances of uncoordinated transmission in MAC phase with degree distribution $\Lambda_{\mathrm{b}}(x) = 0.25x^2 + 0.6x^3 + 0.15x^8$.

achieves throughput of 0.75 packets/slot practically and 0.89 packets/slot asymptotically.

The average BER performances of MAC phase are evaluated over AWGN channels. We consider MWMRN-2C with 50 users for each cluster, the total of which is 100 users. The distance of users to the nearest relay is assumed to be 3/4 of the distance to the other relay, $\delta_d = (3/4)\delta_{\mathrm{ref}}$. For the *physical* encoder we consider convolutional codes $C\ [3, 2]_8$ serially concatenated with unity rate doped-accumulator ACC. Fig. 5.8 shows the average BER performances of each groups in every relays. It is shown that the BER performances of the users to the nearest relay is better compared to that of to another relay. However, the networks suffer from early error-floor as the impact of PLR floor shown in Fig. 5.6. This error-floor condition can later be solved by employing IDM algorithm in the SIC since the appearance probability of stopping sets is significantly reduced by applying IDM algorithm.

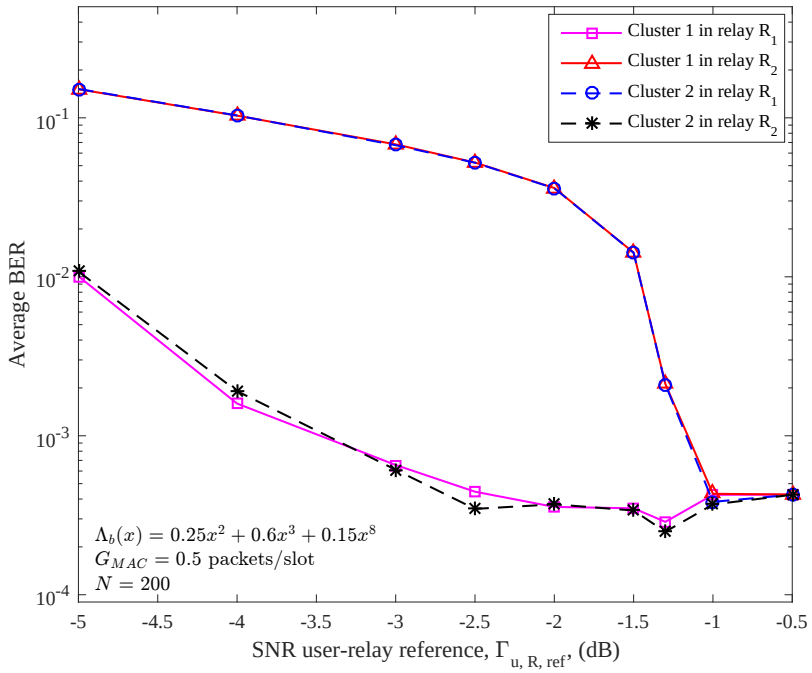

Fig. 5.8: BER performances of MWMRN-2C in MAC phase.

5.1.3 Broadcast Channel (BC) Phase

5.1.3.1 Transmission Strategy in BC Phase

Since mDF relaying protocol is assumed, the relays keep forwarding the decoded data to all users even though error is detected. This strategy is more advantageous when source correlation is exploited.

The transmitter structure of relay $\mathcal{R}_r$ is shown in Fig 5.9, where $\pi_{r,0,i}$ is introduced to exploit the source correlation. The decoded data of user u_i, $\tilde{b}_{r,i}$, is first interleaved using random interleaver $\pi_{r,0,i}$. The interleaved version of $\tilde{b}_{r,i}$ is

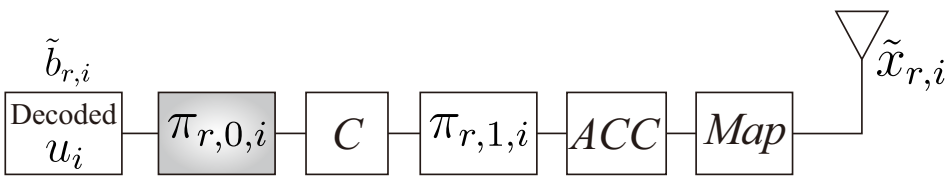

Fig. 5.9: Transmitter structure of relay $\mathcal{R}_r$.

encoded using encoder C, and again interleaved using random interleaver $\pi_{r,1,i}$, and then doped-accumulated using ACC. The outputs of ACC are mapped to BPSK symbols $\tilde{x}_{r,i}$.

The transmission in BC phase is performed via the last $2M$ TSs of the transmission *frame*, because we assume that one relay requires one TS to transmit one user's message. However, this $2M$ TSs can be significantly reduced when higher order modulation is applied. The relays broadcast their messages in turn. At TS s_j, $j = N + (2i - 1)$, relay $\mathcal{R}_1$ broadcasts the message corresponding to u_i, $\tilde{x}_{r,i}$, while relay $\mathcal{R}_2$ broadcasts $\tilde{x}_{r,i}$ via next TS, s_{j+1}. The signals received by user u_m, $m \in \{1, 2, ..., M\}$, is expressed by

$$\tilde{y}_{m,j} = \sqrt{\Gamma_{\mathcal{R}_1,u_m}}\tilde{x}_{1,i} + z_m \tag{5.18}$$

$$\tilde{y}_{m,j+1} = \sqrt{\Gamma_{\mathcal{R}_2,u_m}}\tilde{x}_{2,i} + z_m, \tag{5.19}$$

where z_m is the zero-mean Gaussian noise at user u_m with variance $\sigma_m^2 = 1$.

5.1.3.2 Final Joint Decoding Strategy

After receiving two signals $\tilde{y}_{m,j}$ and $\tilde{y}_{m,j+1}$ from relay $\mathcal{R}_1$ and $\mathcal{R}_2$, respectively, user u_m performs joint decoding between two SCC decoders corresponding to the relays as described in Fig. 5.10. There are two main iterative loops: *horizonal iteration* (HI) and *vertical iteration* (VI). Decoding is started from HI loop that corresponds to the iterative processing in SCC decoders consisting of decoder D_r, interleaver $\pi_{r,1,i}$ and de-interleaver $\pi_{r,1,i}^{-1}$, where $r \in \{1, 2\}$, decoder of doped-accumulator $DACC$, and demapper DM. Extrinsic information in the form of LLRs are exchanged during HI loop. After some iterations in HI loop, joint decoding between decoders D_1 and D_2 via VI loop is performed. Decoders D_1 and D_2 are exchanging extrinsic LLRs via interleaver $\pi_{r,0,i}$, de-interleaver $\pi_{r,0,i}^{-1}$, and f_c function. The f_c function role is very important to prevent error propagation during decoding process [12], the LLRs output of which are given by

$$L_{\text{out}} = f_c(L_{\text{in}}, \epsilon_i) = \log \frac{(1 - \epsilon_i)e^{L_{\text{in}}} + \epsilon_i}{(1 - \epsilon_i) + \epsilon_i e^{L_{\text{in}}}}, \tag{5.20}$$

where ϵ_i is correlation factor of decoded messages in relays $\mathcal{R}_1$ and $\mathcal{R}_2$ corresponding to user u_i and L_{in} is LLRs input of f_c function.

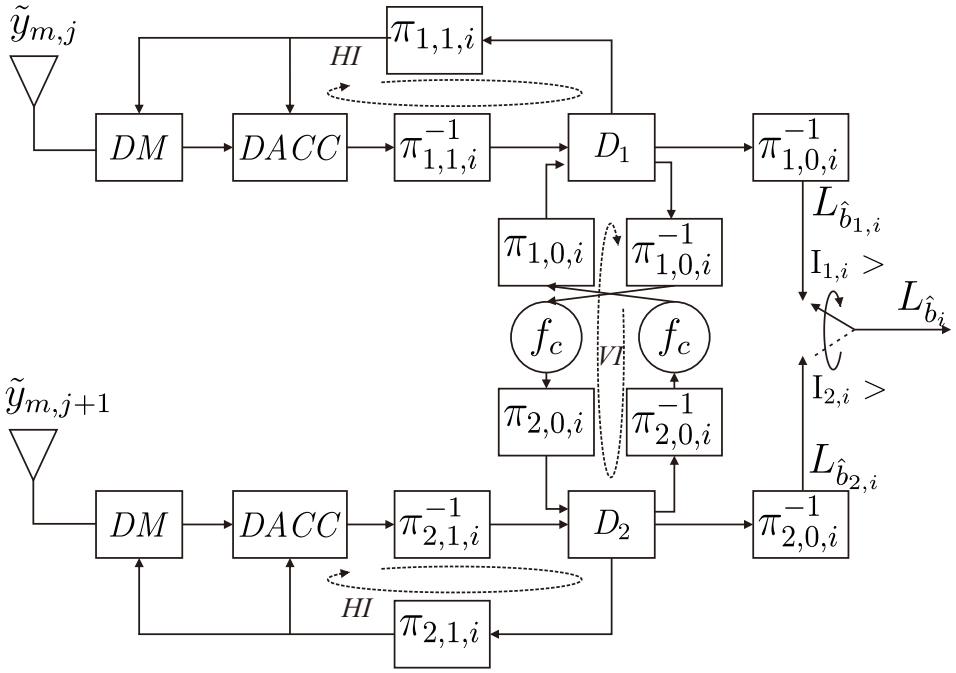

Fig. 5.10: Receiver structure at user u_m to jointly decode the received messages corresponding to user u_i from $\mathcal{R}_1$ and $\mathcal{R}_2$.

In the final step, the selection of *host decoder* (either D_1 or D_2), of which the LLR outputs are used for the final decision, is of significant importance to ensure the best decoding results. We propose a *host decoder selection* based on mutual information (MI) calculated by the relays. The relay $\mathcal{R}_r$ calculates MI of decoded messages corresponding to user u_i, $\mathrm{I}_{r,i}$, then transmit it to all users, using a specific field in the packet header of every transmission. We choose the decoder associated with the relay having the highest MI as the *host decoder*. The $\mathrm{I}_{r,i}$ is calculated using

$$\mathrm{I}_{r,i} \approx 1 - \frac{1}{\mathcal{K}} \sum_{\kappa=1}^{\mathcal{K}} H_b \left(\frac{e^{\frac{+|L_{\tilde{b}_{r,i,\kappa}}|}{2}}}{e^{\frac{+|L_{\tilde{b}_{r,i,\kappa}}|}{2}} + e^{\frac{-|L_{\tilde{b}_{r,i,\kappa}}|}{2}}} \right), \tag{5.21}$$

where $\mathcal{K} = T_s R_P$ is length of message b_i, $H_b(\cdot)$ is binary entropy function, and $L_{\tilde{b}_{r,i}}$ is LLRs value of decoded data $\tilde{b}_i$ at relay $\mathcal{R}_r$, as used in [25]. This equation is practical because the relays do not need to know the original message b_i to estimate the mutual information. This equation may not be the real mutual information as defined in many literature of information theory. However, it is very helpful and confirmed to be effective in practice.

Finally, hard decision is carried out based on $L_{\hat{b}_i}$, which is the de-interleaved version of the *host decoder* outputs.

5.1.3.3 Source Correlation Estimation

The decoded messages corresponding to user u_i in both relays are correlated since they are originally sent from the same source. This source correlation is one of important parameters for the proposed joint decoding strategy to reduce both error-rate and required transmit power.

In a perfect situation, when relays know the error probability of the decoded messages corresponding to user u_i, the correlation factor ϵ_i can be calculated prior to final joint decoding [26]. Technically, when user u_i transmits binary message b_i to the network, after N TSs, it is decoded as $\tilde{b}_{1,i}$ in relay $\mathcal{R}_1$ and $\tilde{b}_{2,i}$ in relay $\mathcal{R}_2$ with error probability $\epsilon_{1,i}$ and $\epsilon_{2,i}$, respectively. Once the destination knows the value of $\epsilon_{1,i}$ and $\epsilon_{2,i}$, the perfect correlation factor is calculated as

$$\epsilon_{\text{perfect},i} = \epsilon_{1,i} + \epsilon_{2,i} - 2\epsilon_{1,i}\epsilon_{2,i}. \tag{5.22}$$

However, in practice, the destination (each user) has no knowledge of error probability of the decoded messages. To solve this problem, we propose *online* estimation of correlation factor for user u_i *during* the final joint decoding process using

$$\epsilon_{\text{est},i} = \frac{1}{\mathcal{L}} \sum_{l=1}^{\mathcal{L}} \frac{\exp\left(L_{\hat{b}_{1,i}}\right) + \exp\left(L_{\hat{b}_{2,i}}\right)}{\left(1 + \exp\left(L_{\hat{b}_{1,i}}\right)\right)\left(1 + \exp\left(L_{\hat{b}_{2,i}}\right)\right)}, \tag{5.23}$$

where $L_{\hat{b}_{r,i}}$ is *a posteriori* LLRs of $\hat{b}_i$ from the decoder associated to relay $\mathcal{R}_r$, $\mathcal{L}$ is number of reliable *a posteriori* LLRs selected from LLRs with absolute values greater than threshold $\mathcal{T} = 4$. The results are shown in Fig. 5.11 with $\delta_d = 0.75\delta_{\text{ref}}$.

Fig. 5.11 shows the average BER performances in BC phase for both cases: when source correlation is known (perfect) and estimated (*online*) by the final joint decoder. Please note that X-axis is SNR from relay to the users with distance δ_{ref}, $\Gamma_{\mathcal{R},u,\text{ref}}$. In the lower SNR, the performance difference is noticeable, but negligible. However, when the SNR is high, around -2.5 dB, both cases have the same performance indicating the accuracy of the proposed online estimation. The results confirm that the proposed *online* estimation of correlation factor is very accurate for the final joint decoding exploiting source correlation.

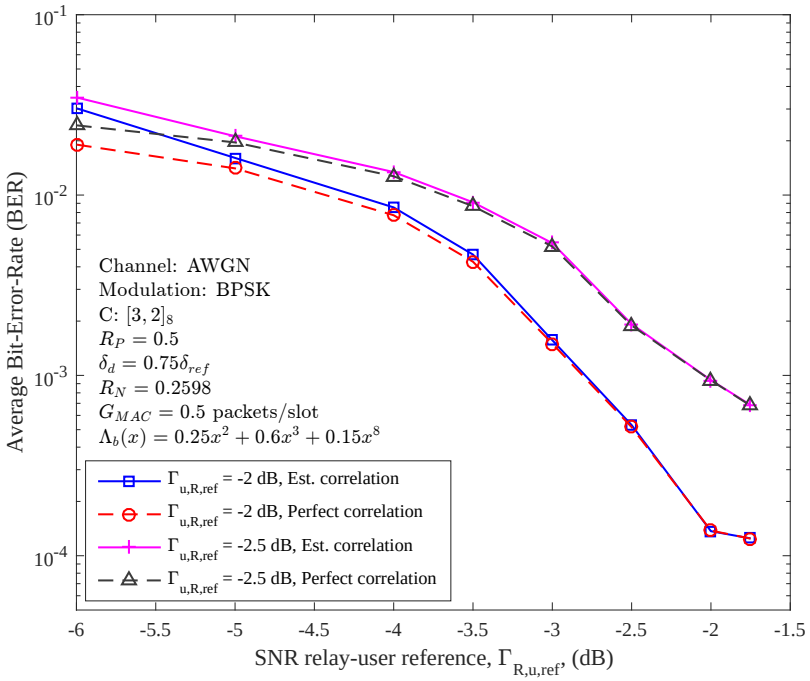

Fig. 5.11: Average BER performance in BC phase using correlation obtained from perfect and *online* estimation.

5.1.4 Performance Evaluations

Computer simulation is conducted to evaluate the performances of MWMRN-2C. We consider in total 100 users that are divided into two clusters of 50 users. The distance from a user to the nearest relay is $\delta_d = (3/4)\delta_{\text{ref}}$. We assume that the transmit power of the relays and users are equal, $P_{\mathcal{R}} = P_u$. Hence, SNR for distance δ_d is expressed by $\Gamma_{\mathcal{R},u,d} = \Gamma_{\mathcal{R},u,\text{ref}} + 4.3978$ and $\Gamma_{\mathcal{R},u,d} = \Gamma_{u,\mathcal{R},d}$.

The channel is assumed to be AWGN channels. Memory-1 convolutional codes $[3, 2]_8$ with half rate is concatenated with doped-accumulator ACC to be used as *physical* encoder. For *network* encoder, we utilize irregular repetition code with degree distribution $\Lambda_{\text{b}}(x) = 0.25x^2 + 0.6x^3 + 0.15x^8$ having average network rate $R_N = 0.2857$. To ensure reliable information exchange in MWMRN-2C, the offered traffic for MAC phase has to be set less than threshold G^*_{MAC}, which is $G^*_{\text{MAC}} = 0.89$ packets/slot for $\Lambda_{\text{b}}(x)$. In this evaluation we choose offered traffic $G_{\text{MAC}} = 0.5$ packets/slot, which exhibits lower PLR floor (see Fig. 5.6).

We focus on the MWMRN-2C performances in terms of average BER and

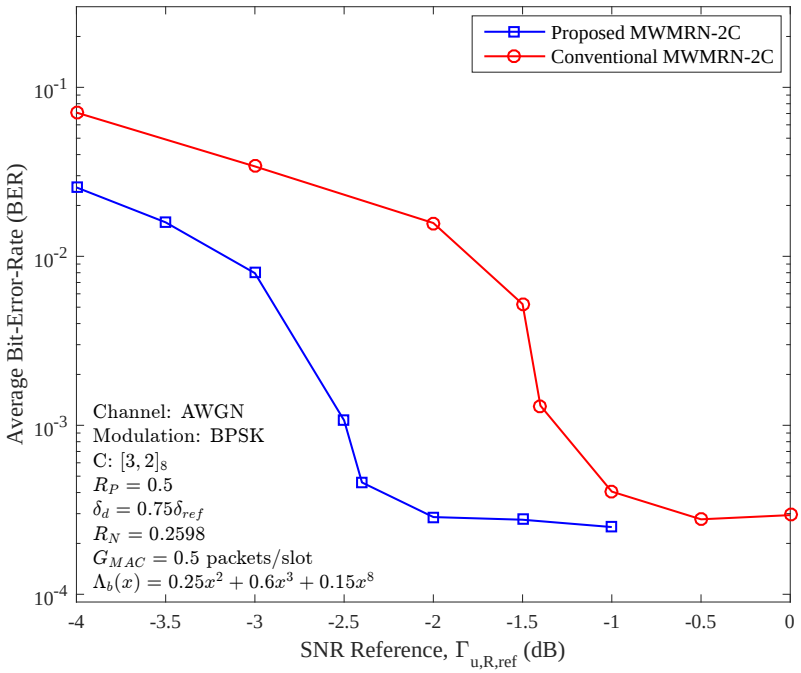

Fig. 5.12: Average BER performances of MWMRN-2C.

throughput performances. As comparison, we also evaluate performances of traditional MWMRN-2C without joint decoding. Moreover, the traditional MWMRN-2C adopts conventional DF relaying scheme, i.e., erroneous messages are not forwarded to all users. However, in the case of both messages in the both relays are erroneous, instead of making BER=0.5, we calculate BER by assuming that one of the messages is forwarded to all users for the fairness. Fig. 5.12 shows the average BER performances with $G_{\mathrm{MAC}} = 0.5$ packets/slot. It is confirmed that the proposed techniques yield better BER performance compared to the conventional MWMRN-2C. In BER of 10^{-2}, 1.25 dB gain is achieved by the proposed technique. We also observe from the figure that the MWMRN-2C suffers from error-floor around 10^{-4}. This error floor is inherited from the uncoordinated transmission as shown in Fig. 5.6.

Fig. 5.13 shows the throughput performances achieved by the proposed and conventional MWMRN-2C. We also plot the maximum throughput to be achieved

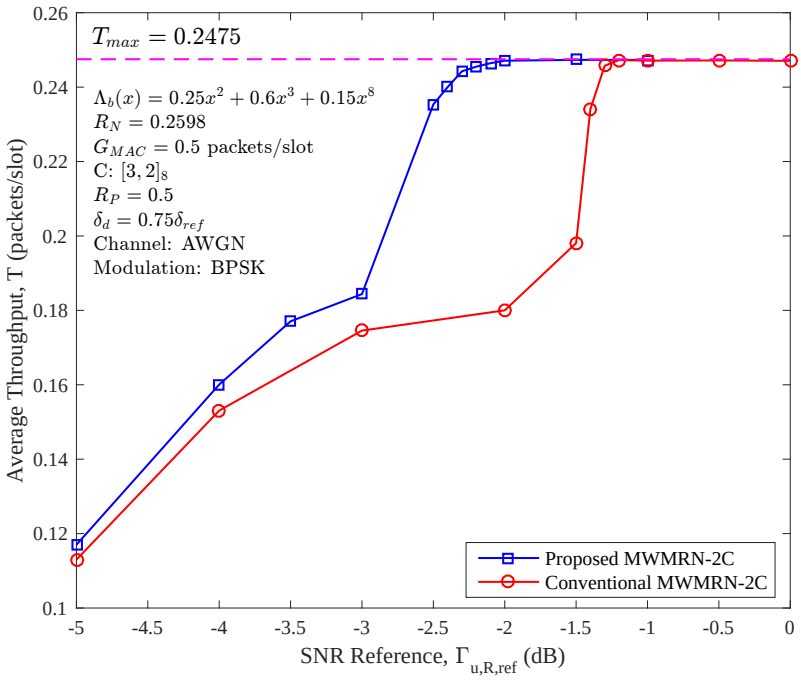

Fig. 5.13: Throughput performances of MWMRN-2C.

by the MWMRN-2C with a certain offered traffic G_{MAC}, which is calculated as

$$T_{\max} = \frac{M-1}{L} = \frac{M-1}{N+2M} \tag{5.24}$$

$$= \frac{(M-1)G_{\text{MAC}}}{M(1+2G_{\text{MAC}})}. \tag{5.25}$$

Since $G = 0.5$ packets/slot is considered, the maximum throughput achieved by the MWMRN-2C under evaluation is $T_{\max} = 0.2475$ packets/slot. It can clearly be seen that the proposed technique achieves maximum throughput with lower SNR. It is around SNR of 2.3 dB that the proposed MWMRN-2C almost achieves $T_{\max}$, while the conventional MWMRN-2C achieves $T_{\max}$ at SNR around 1.2 dB.

5.2 Distributed Multiway Multirelay Networks

This section focuses on more general MWMRN, where arbitrary number of relays are considered to serve massive number of users distributed in an area randomly. We call this networks as distributed multiway multirelay networks (D-MWMRN).

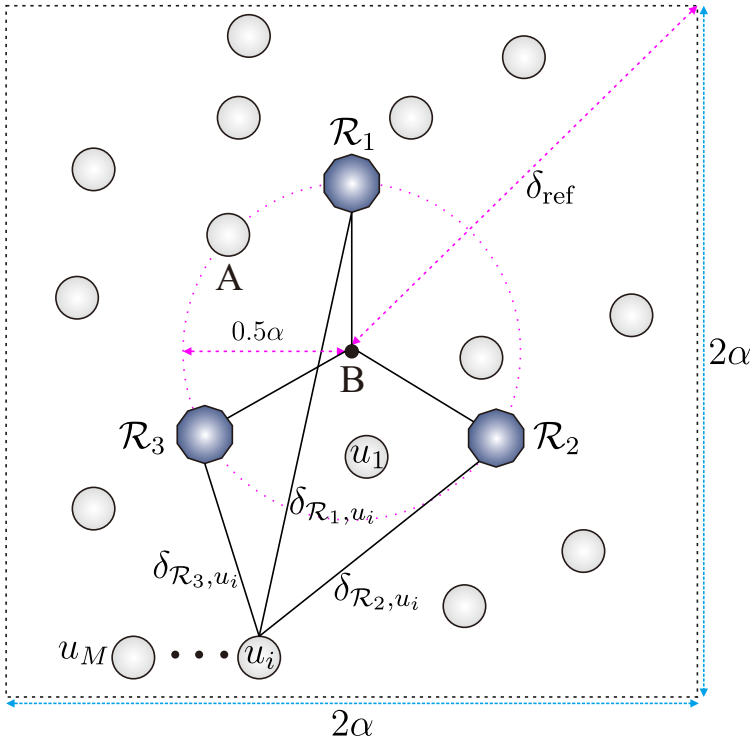

Fig. 5.14: D-MWMRN with $Q = 3$ relays, $\mathcal{R}_1$, $\mathcal{R}_2$ and $\mathcal{R}_3$.

5.2.1 System Model

D-MWMRN consists of M users and Q relays. For $Q = 3$, the system model is illustrated in Fig. 5.14. The randomly distributed users in a square area $2\alpha \times 2\alpha$ with diagonal $2\delta_{\text{ref}}$ expect to exchange information among themselves with the help of Q relays. Each user wants to decode information from the other $(M-1)$ users, by assuming that all the users have connection to all relays. The distance between relay $\mathcal{R}_r$, $r \in \{1, ..., Q\}$, and user u_i, $i \in \{1, ..., M\}$, is $\delta_{\mathcal{R}_r,u_i}$. We assume that the relays are the only communication enablers in the networks, where no direct link between any users.

The transmit power of users and relays are assumed to be equal. Distance δ_{ref}, which is the distance from a corner point of the square to the center (point B) in Fig. 5.14, is selected as the reference. This distance has SNR Γ_{ref}. Thus, SNR for the link between $\mathcal{R}_r$ and user u_i is defined as

$$\Gamma_{u_i,\mathcal{R}_r} = \Gamma_{\mathcal{R}_r,u_i} = \left(\frac{\delta_{\text{ref}}}{\delta_{\mathcal{R}_r,u_i}}\right)^{\gamma} \Gamma_{\text{ref}}, \tag{5.26}$$

where γ is path-loss exponent assumed to be $\gamma = 3.52$.

Half-duplex mode is assumed in the transmission scheme with perfect frame and slot synchronizations. All users conduct information exchange within one *frame* composed of $L = (N + QM)$ time slots (TS), where each TS has equal time duration T_s. The first N of L TSs are utilized in MAC phase, while the remaining QM TSs are used in BC phase.

Similar to the MWMRN-2C, offered traffic of MAC phase in D-MWMRN is given by

$$G_{\text{MAC}} = \frac{M}{N}, \tag{5.27}$$

which is an important parameter for networks throughput optimization. On the other hand, offered traffic in BC phase is fixed to $G_{\text{BC}} = \frac{M-1}{QM}$.

5.2.2 Multiple Access Channel (MAC) Phase

To effectively handle the transmission of massive number of users, uncoordinated transmission strategy is proposed for D-MWMRN. In the first N TSs of transmission *frame*, all users randomly transmit their information to the relays without coordination with the other users. The details of transmission strategy is quite similar to what was explained in Subsubsection 5.1.2. After N TSs, relay $\mathcal{R}_r$, $r \in \{1, 2, ..., Q\}$ receives

$$Y_r = AX_r + Z_r, \tag{5.28}$$

with

$$Y_r = [y_{r,1}\ y_{r,2}\ ...\ y_{r,N}]^T, \tag{5.29}$$

$$X_r = [\sqrt{\Gamma_{u_1,\mathcal{R}_r}}x_1\ \sqrt{\Gamma_{u_2,\mathcal{R}_r}}x_2\ ...\ \sqrt{\Gamma_{u_M,\mathcal{R}_r}}x_M]^T, \tag{5.30}$$

$$Z_r = [z_{r(1)}\ z_{r(2)}\ ...\ z_{r(N)}]^T, \tag{5.31}$$

$$A = \begin{bmatrix} a_{1,1} & a_{1,2} & ... & a_{1,M} \\ a_{2,1} & a_{2,2} & ... & a_{2,M} \\ ... & .... & a_{j,i} & ... \\ a_{N,1} & a_{N,2} & ... & a_{N,M} \end{bmatrix}. \tag{5.32}$$

5.2.2.1 Proposed Decoding Strategy in Relays

In the conventional techniques, decoding in the relays is performed as follows. It is started by finding degree $d = 1$ slot node, where only one user transmits a message. The *physical* decoding using SCC decoder is performed in this slot node. The results are passed to the connected user node to be used in user node *network* decoding. The user node then passes the results to the connected slot nodes. Subsequently, SIC is performed by subtracting the decoded messages from the composite signals in the connected slot nodes. The decoding stops when no more degree $d = 1$ slot node found.

To let the decoding process progresses further, we propose the use of IDM algorithm that has capability of decoding two messages from two users simultaneously. When no more degree $d = 1$ slot node found, instead of stopping the decoding process, we continue by finding degree $d = 2$ slot node, where two users simultaneously transmit their messages. The IDM algorithm is employed in the slot node *physical* decoding to decode the messages from two users simultaneously. The results are then passed to the connected user nodes to be used in user nodes *network* decoding. The users nodes subsequently transfer the results to the connected slot nodes to be used in interference cancellation. The aforementioned processes are repeated until there is no more degree $d = 1$ or $d = 2$ slot node found or until maximum iteration reached.

The employment of IDM algorithm increases the probability of successful decoding in the relays. This technique allows the systems to work very well even though number of TSs is less than number of users in MAC phase, $N < M$, yielding significant improvement on the total throughput.

5.2.2.2 Analysis and Performance Evaluations in MAC Phase

Since irregular repetition codes is employed as *network* encoder and IDM algorithm is incorporated into SIC, EXIT functions of user nodes and slot nodes are given by

$$f_u(p_{\ell-1}) = \sum_{h=2}^{n_c} \lambda_h p_{\ell-1}^{h-1}, \tag{5.33}$$

$$f_s(q_\ell) = 1 - \left(1 + q_\ell \frac{G_{\mathrm{MAC}}}{R_N}\right) e^{-q_\ell \frac{G_{\mathrm{MAC}}}{R_N}}, \tag{5.34}$$

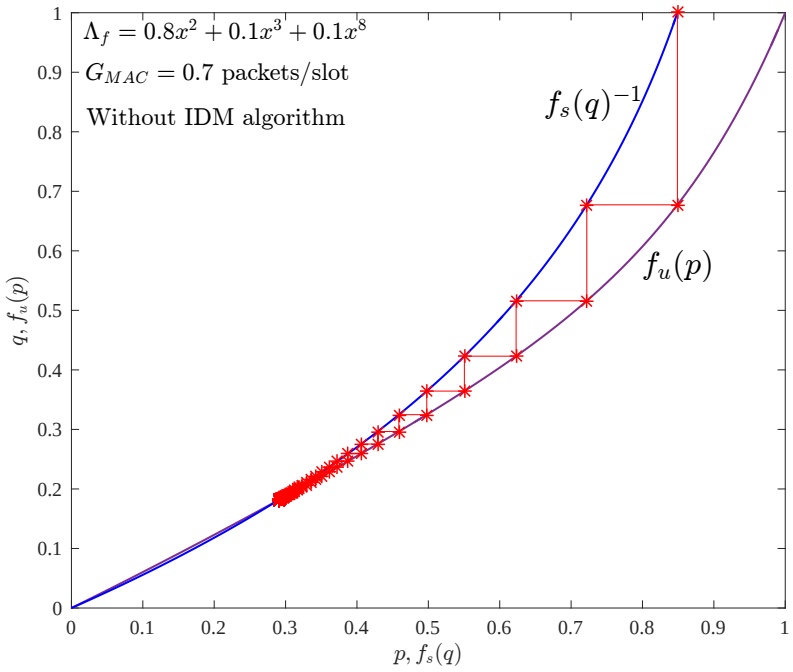

Fig. 5.15: EXIT chart of MAC phase transmission scheme with degree distribution Λ_{f} when IDM algorithm is *not* incorporated into SIC process.

respectively. Now we use degree distribution of user node $\Lambda_{\mathrm{f}} = 0.8x^2 + 0.1x^3 + 0.1x^8$ with $R_N = 0.3704$ in MAC phase transmission of D-MWMRN. When IDM algorithm is not incorporated into SIC process, the EXIT chart of the networks is shown in Fig. 5.15. Even with offered traffic only $G_{\mathrm{MAC}} = 0.7$ packets/slot, the decoding process does not converge to point $(0, 0)$. This is because the threshold G^*_{MAC} is only 0.618 packets/slot, which can only be achieved asymptotically with very large N ($N \to \infty$).

On the other hand, when IDM algorithm is incorporated into SIC process, significant throughput gain can be achieved. Fig. 5.16 shows the decoding convergence in MAC phase with IDM algorithm using the same degree distribution Λ_{f}. Even though with higher offered traffic ($G_{\mathrm{MAC}} = 1.82$ packets/slot), the trajectory of EXIT chart passes through *small tunnel* between two curves and reaches point $(0, 0)$ indicating that the decoding process is successful with high probability. The corresponding threshold is $G^*_{\mathrm{MAC}} = 1.822$ packets/slot, which is almost three times higher compared to the case of without IDM algorithm.

Figs. 5.17 and 5.18 show the results of simulations conducted under high SNR

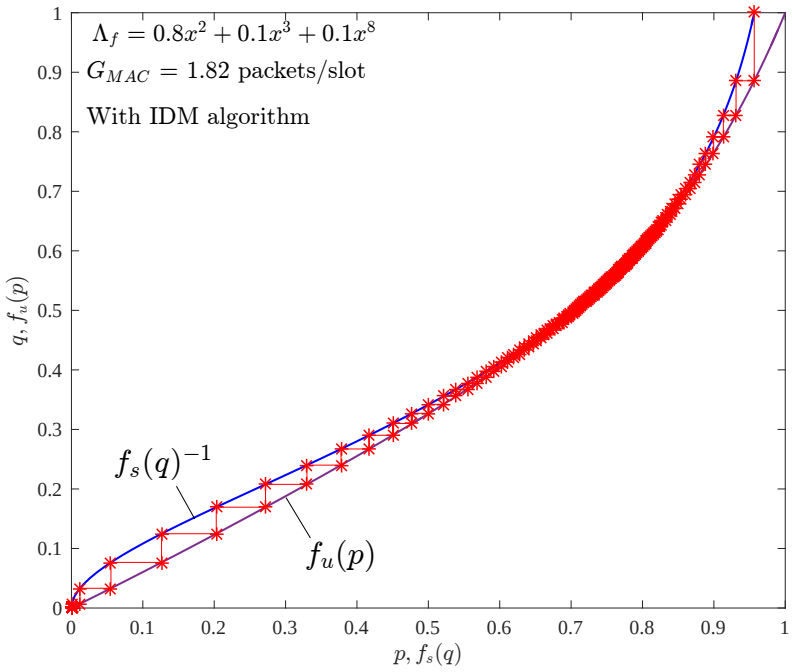

Fig. 5.16: EXIT chart of MAC phase transmission scheme with degree distribution Λ_{f} when IDM algorithm is incorporated into SIC process.

assumption for D-MWMRN with user node degree distribution $\Lambda_{\mathrm{f}}(x) = 0.8x^2 + 0.1x^3 + 0.1x^8$. Number of TSs is fixed to $N = 200$, while number of users is varying depends on the value of G_{MAC}, $M = NG_{\mathrm{MAC}}$.

In Fig. 5.6, the superiority of the proposed decoding strategy in terms of PLR performance is shown. With $\Lambda_{\mathrm{f}}(x)$, higher traffic can be reliably offered by the proposed technique. Moreover, it provides very low PLR floor of 10^{-4} because the appearance probability of stopping set is significantly reduced. The proposed technique also outperforms the conventional technique in terms of throughput performances. It achieves throughput of 1.6 packets/slot which is almost three times higher compared to that of conventional technique even though with finite-length setting of $N = 200$. The throughput improvement in MAC phase has significant contribution to the improvement of total networks throughput.

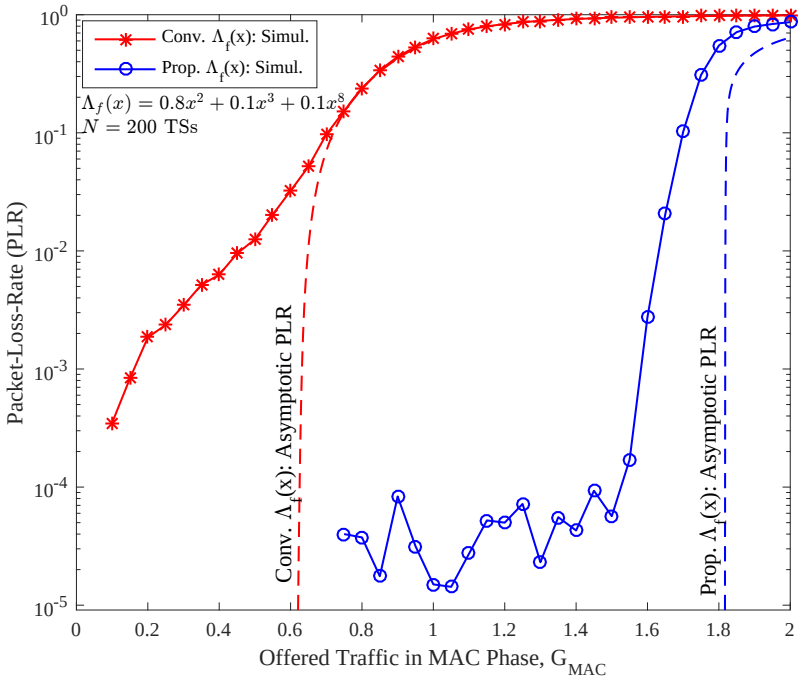

Fig. 5.17: PLR performances in MAC phase.

5.2.3 Broadcast Channel (BC) Phase

5.2.3.1 Transmission Strategy in BC Phase

After all data from users are fully decoded, relay $\mathcal{R}_r$, $\forall r \in \{1, 2, ..., Q\}$, estimates mutual information (MI) of the decoded data of user u_i, $\mathrm{I}_{r,i}$, using (5.21). The $\mathrm{I}_{r,i}$ is then transmitted by relay $\mathcal{R}_r$ to all users, using a specific field in packet header at every transmission. The $\mathrm{I}_{r,i}$ is important for every users to ensure the best results in the final joint decoding.

The transmitter structure of relay $\mathcal{R}_r$ in BC phase is similar to the case of MWMRN-2C illustrated in Fig 5.9. The decoded data $\tilde{b}_{r,i}$ is first interleaved using random interleaver $\pi_{r,0,i}$, encoded using encoder C, and again interleaved using random interleaver $\pi_{r,1,i}$, and then doped-accumulated using ACC. The output of ACC is modulated by Map to produce message $\tilde{x}_{r,i}$.

All messages are transmitted via the last QM TSs of the transmission *frame* sequentially. At TS s_{t+r}, where $t = N + Q(i-1)$, relay $\mathcal{R}_r$ broadcasts the message corresponding to user u_i, $\tilde{x}_{r,i}$. The signals received by user u_m, $\forall m \in \{1, 2, ..., M\}$,

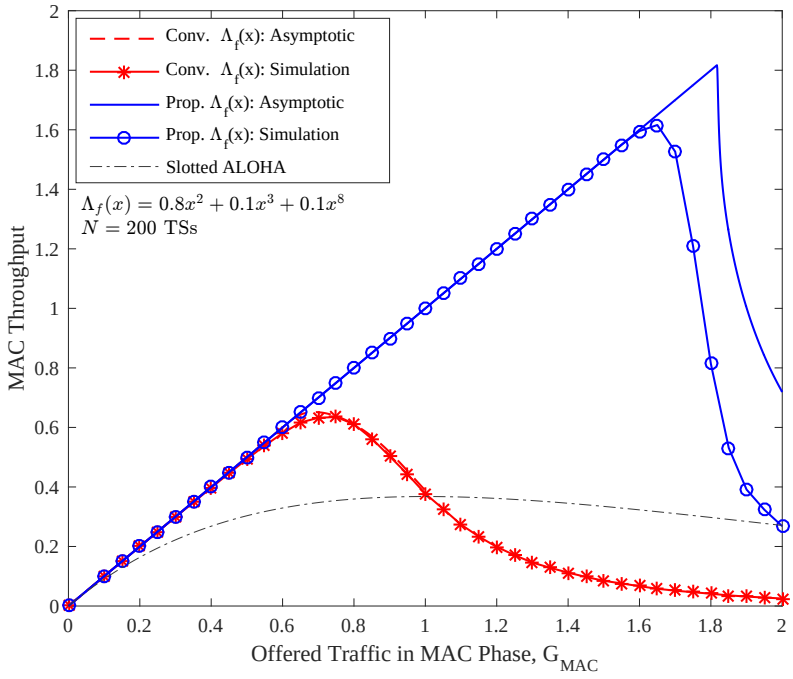

Fig. 5.18: Throughput performances in MAC phase.

in BC phase is expressed as

$$\tilde{y}_{m,t+r} = \sqrt{\Gamma_{\mathcal{R}_r,u_m}}\tilde{x}_{r,i} + z_m \tag{5.35}$$

where z_m is the zero-mean Gaussian noise at user u_m with variance $\sigma_m^2 = 1$.

5.2.3.2 Proposed General Joint Decoding Strategy

Fig. 5.19 describes the proposed final joint decoding structure, which is a generalization of joint decoding structure of MWMRN-2C presented in Section. 5.1. It consists of Q *HI* loops corresponding to the number of relays. In each *HI* loop, demapper *DM* together with decoder of doped-accumulator *DACC* are exchanging extrinsic LLRs with decoder D_r through interleavers and de-interleavers. After some iterations in *HI* loop, the *VI* loop is performed by exchanging extrinsic LLRs between all decoders D_r through interleavers, de-interleavers, $f_{c,r}$ functions, and *VN* decoder.We call it *VN* decoder because of its similarity to variable node (VN) decoder in low-density parity-check (LDPC) codes.

The source correlation of the messages of user u_i to be exploited using $f_{c,r}$

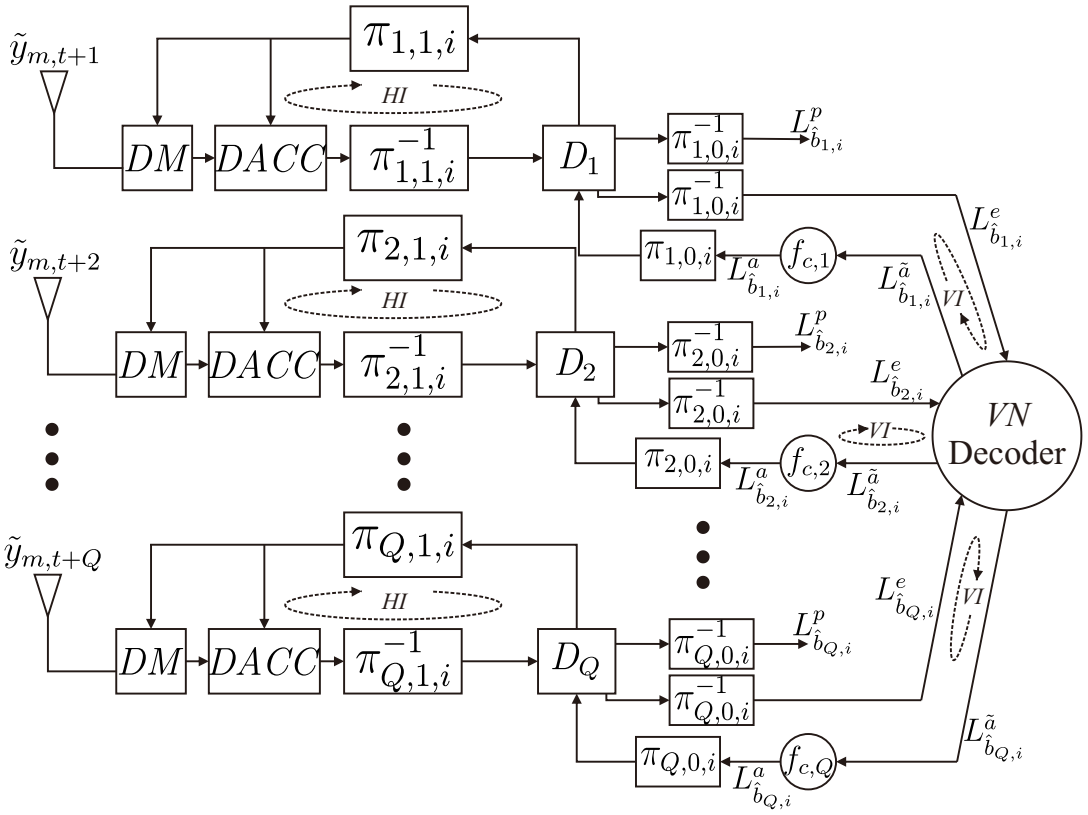

Fig. 5.19: Block diagram of final decoding at user u_m to decode information of user u_i.

function is

$$\epsilon_{r,i} = \frac{1}{\mathcal{L}} \sum_{l=1}^{\mathcal{L}} \frac{\exp\left(L^{p}_{\hat{b}_{r,i}}\right) + \exp\left(L^{pc}_{\hat{b}_{r,i}}\right)}{(1+\exp\left(L^{p}_{\hat{b}_{r,i}}\right))(1+\exp\left(L^{pc}_{\hat{b}_{r,i}}\right))}, \tag{5.36}$$

where

$$L^{pc}_{\hat{b}_{r,i}} = \sum_{\kappa=1,\kappa\neq r}^{Q} L^{p}_{\hat{b}_{\kappa,i}}, \tag{5.37}$$

$L^{p}_{\hat{b}_{r,i}}$ is *a posteriori* LLRs of the decoded messages $\hat{b}_i$ from D_r, and $\mathcal{L}$ is number of reliable *a posteriori* LLRs, which are selected from LLRs having absolute value greater than threshold $\mathcal{T} = 4$. The threshold $\mathcal{T} = 4$ is obtained empirically as [12].

The extrinsic LLRs from all decoders are passed to the *VN* decoder to be used in *VI* loop. The outputs of *VN* decoder for decoder D_r is given by

$$L^{\tilde{a}}_{\hat{b}_{r,i}} = \sum_{\kappa=1,\kappa\neq r}^{Q} L^{e}_{\hat{b}_{\kappa,i}}, \tag{5.38}$$

which is then used by $f_{c,r}$ function to provide *apriori* LLRs for decoder D_r

$$\begin{aligned} L^{a}_{\hat{b}_{r,i}} &= f_{c,r}(L^{\tilde{a}}_{\hat{b}_{r,i}}, \epsilon_{r,i}) \\ &= \log \frac{(1-\epsilon_{r,i})\exp(L^{\tilde{a}}_{\hat{b}_{r,i}}) + \epsilon_{r,i}}{(1-\epsilon_{r,i}) + \epsilon_{r,i}\exp(L^{\tilde{a}}_{\hat{b}_{r,i}})}. \end{aligned} \tag{5.39}$$

In the final step, *host decoder*, of which the outputs are used for the final decision, is selected based on MI calculated by the relays. As illustrated in Fig. 5.10, there are Q possible *a posteriori* LLRs $L^{p}_{\hat{b}_{r,i}}$ candidates to be used for final decision. The decoder of the relay with the highest MI is chosen as the *host decoder*, i.e.,

$$L_{\hat{b}_i} = L^{p}_{\hat{b}_{r,i}}, \tag{5.40}$$

where $I_{r,i} = \max\{I_{1,i}, ..., I_{Q,i}\}$. Hard decision is then performed based on $L_{\hat{b}_i}$ to obtain $\hat{b}_i$.

5.2.4 Performances Evaluations

We evaluate performances of D-MWMRN via computer simulations for 100 users. The users are located randomly in a square area of $2\alpha \times 2\alpha$ (implies $\delta_{\text{ref}} = \alpha\sqrt{2}$), except two of them are intentionally located in locations A and B as shown in Fig. 5.14. Without loss of generality, the relays are located as follows.[7] In case of $Q = 1$, the relay is placed in the center of the square (location B in Fig. 5.14) for the evaluations purpose. When $Q \geq 2$, the relays are located structurally in locations that have distances $\delta_{\mathcal{R}_r,B} = 0.5\alpha$ from the center (point B). For the sake of fairness, we investigate the performances of a user in a location that has same distances to all the relays. Particularly, in the case of $Q = 1$, we investigate the performance of the user in location A that has distance 0.5α from the relay, while for $Q \geq 2$, we investigate the performances of the user located in B, which has distances 0.5α to all relays.

The simulations are carried out under AWGN channels. Memory-1 convolutional codes $[3, 2]_8$ with half rate is used as encoder C that is serially concatenated with doped-accumulator ACC via an interleaver. User nodes degree distribution $\Lambda_{\text{f}}(x) = 0.8x^2 + 0.1x^3 + 0.1x^8$ is adopted for both the proposed and the conven-

[7] The location of the relays can be optimized based on the distribution of users location. However, this optimization is out of the scope of this thesis.

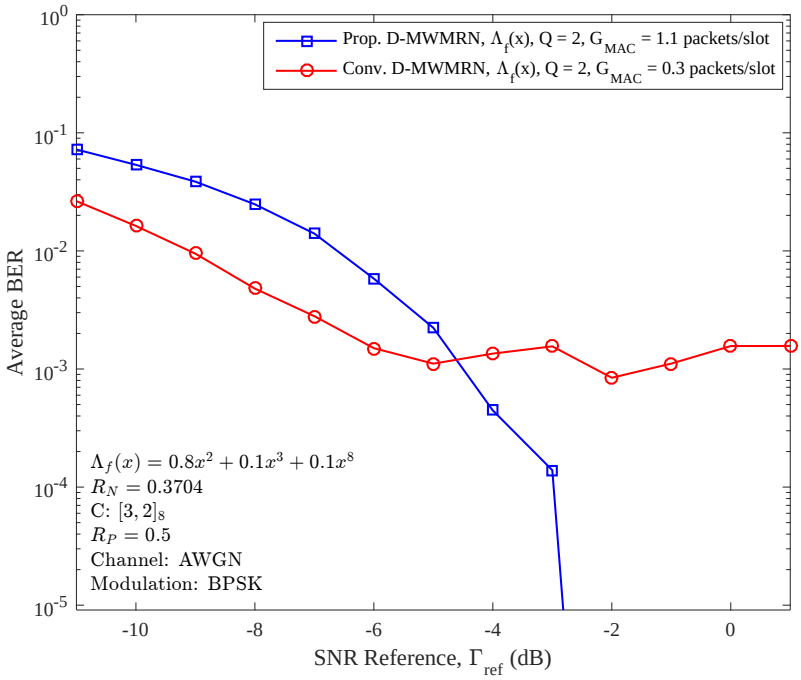

Fig. 5.20: Average BER performances of D-MWMRN with $Q = 2$.

tional D-MWMRN. To ensure reliable communications, the offered traffic must be set less than the asymptotic limit (see Fig. 5.17). For the fairness, we set G_{MAC} for the proposed D-MWMRN to 0.7 from its asymptotic limit, while for the conventional D-MWMRN, G_{MAC} is 0.3 away from its asymptotic limit. Therefore, for the proposed D-MWMRN we set $G_{\text{MAC}} = 1.1$ packets/slot, while for the conventional D-MWMRN we set $G_{\text{MAC}} = 0.3$ packets/slot. The mDF relaying scheme and final joint decoding are only considered in the proposed D-MWMRN.

The results in terms of average BER performances of D-MWMRN with $Q = 2$ relays is shown in Fig. 5.20. In low SNR regime (below -5 dB), the proposed techniques provide slightly worse performance compared to the conventional D-MWMRN. This is as a penalty of using IDM algorithm in SIC, because when SNR is too low, the IDM algorithm is unable to completely separate two different messages. However, in higher SNR, it is clearly shown that the proposed techniques yield excellent average BER performance, where error-floor is unseen below 10^{-5}, while the conventional D-MWMRN suffers from high error-floor as a consequence of higher PLR in MAC phase (see Fig. 5.17).

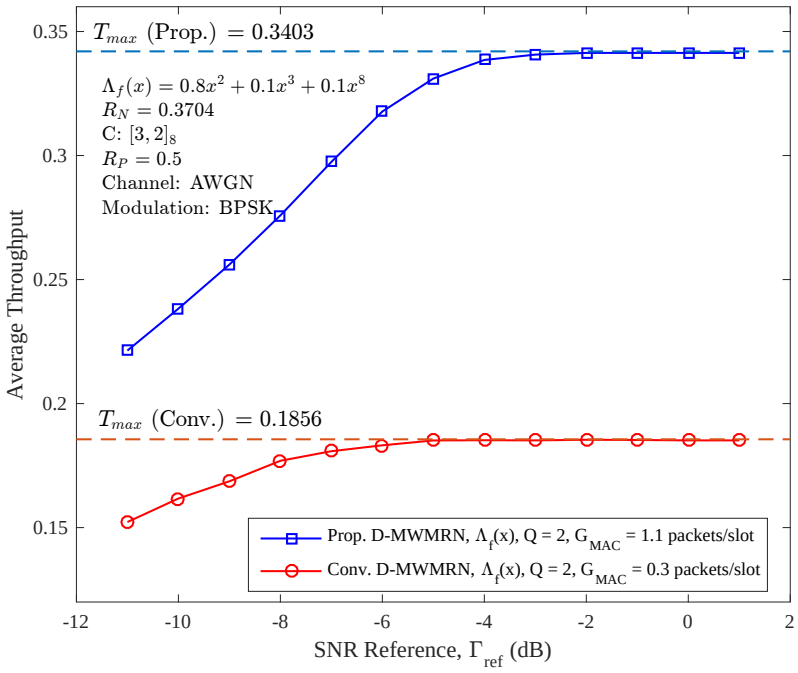

Fig. 5.21: Average throughput performances of D-MWMRN with $Q = 2$.

The throughput performances of D-MWMRN with $Q = 2$ relays are shown in Fig. 5.21. As a reference, the maximum achievable throughput of D-MWMRN with a particular offered traffic G_{MAC} is also shown in Fig. 5.21. For arbitrary number of relays and given G_{MAC}, the maximum throughput is defined as

$$T_{\max} = \frac{M-1}{L} = \frac{M-1}{N+QM} \tag{5.41}$$

$$= \frac{(M-1)G_{\text{MAC}}}{M(1+QG_{\text{MAC}})}. \tag{5.42}$$

We can observe in Fig. 5.21 that the proposed D-MWMRN offers higher throughput compared to the conventional D-MWMRN in the whole range of SNR.

From Figs. 5.20 and 5.21, we conclude that the use of IDM algorithm in MAC phase and joint decoding in BC phase provides significant contribution to the enhancement of BER and throughput performances.

To show the effectiveness of using several relays in D-MWMRN, we evaluate average BER and average throughput performances of the networks with $Q = \{1, 2, 3, 4\}$ relays, of which the results are shown in Figs. 5.22 and Fig. 5.23,

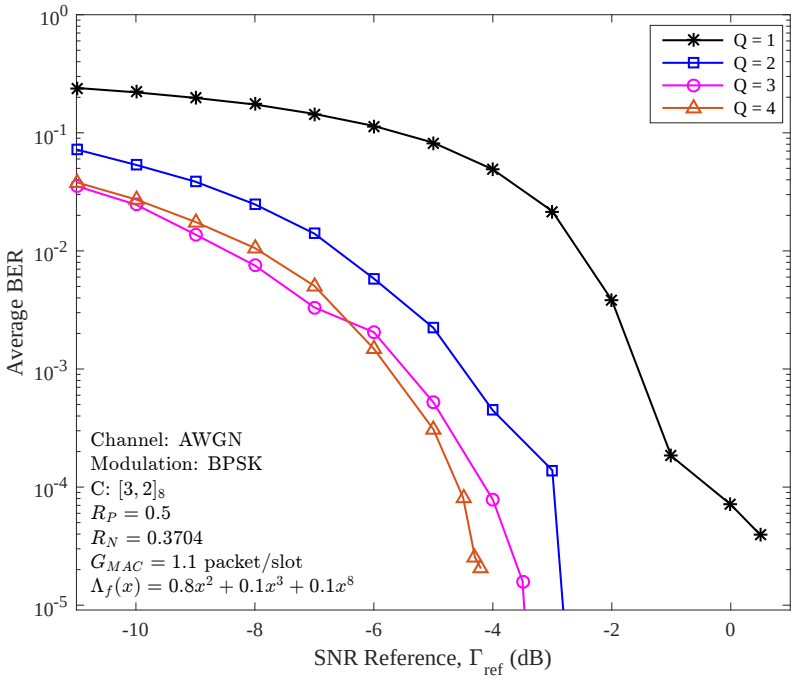

Fig. 5.22: Average BER performances of the proposed D-MWMRN with multiple Q relays.

respectively. In Fig. 5.22, it is shown that D-MWMRN with $Q = 2$ achieves significant power gain around 3 dB compared to D-MWMRN with $Q = 1$. While D-MWMRNs with $Q = 3$ and $Q = 4$ achieve 3.5 dB and 4 dB gain compared to D-MWMRN with $Q = 1$. The power gain provided by multiple relays increases as the number of relays increases. However, when $Q \geq 3$, the achieved gain is not significant.

We also investigate the throughput performances to show the impacts of using multiple relays since the number of required TSs is also determined by the number of relays. Fig. 5.23 shows the average throughput performances evaluated at SNR -12 dB to 0 dB. Since a fixed transmission scheduling is considered for BC phase, the more relays used, the lower throughput can be achieved by the networks. It is shown in Fig. 5.23 that D-MWMRN with $Q = 1$ offer the highest maximum throughput since only M TSs are required for transmission in BC phase. However, in low SNR environment, D-MWMRN with $Q = 1$ has worse throughput performances compared to the cases of $Q = \{2, 3, 4\}$. This excellent throughput performances is achieved by employing the proposed joint decoding technique.

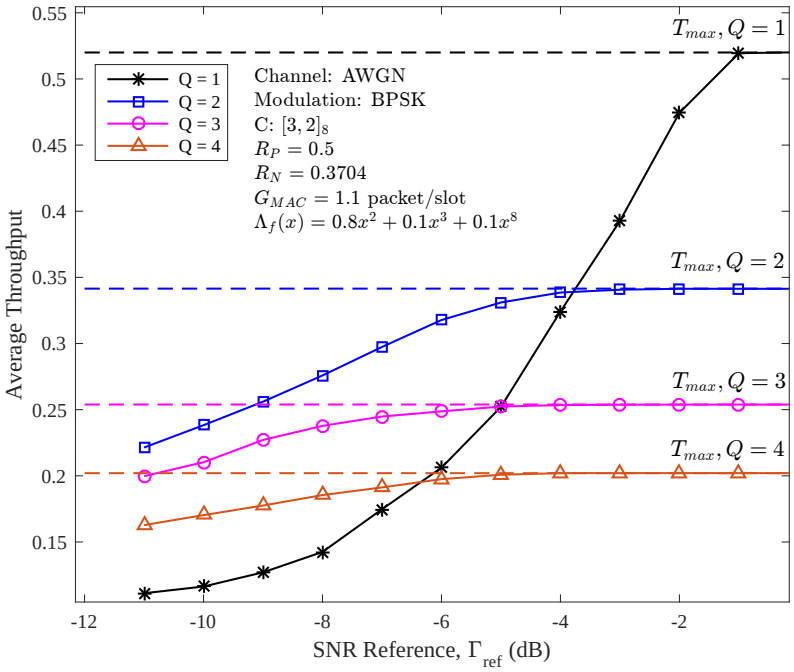

Fig. 5.23: Average throughput performances of the proposed D-MWMRN with multiple Q relays.

From Figs. 5.22 and 5.23, we confirm that D-MWMRN with $Q = 2$ is the most prominent scenario, because it offers significant power gain and also excellent throughput performances in low SNR environment. However, when SNR is high, D-MWMRN with $Q = 1$ is the best choice to reliably serve massive number of users with less complexity.

5.3 Summary

This chapter mainly investigated MWMRNs employing uncoordinated transmission strategy. Two scenarios was considered: MWMRN-2C that serves two separate clusters of users and D-MWMRN that serves randomly distributed users.

In the fist scenario, where all users in two clusters perform information exchange in uncoordinated fashion with the help of two relays, joint decoding that exploits source correlation of the decoded messages in the relays was proposed. *Online* correlation estimation technique was introduced in MWMRN-2C with uncoordinated transmission and confirmed to be effective in practice. Furthermore,

selection of *host decoder*, of which the outputs are used for final decision, based on MI calculated by the relays was proposed. The proposed joint decoding provided significant contribution to the improvement of BER and throughput performances of the networks.

The second scenario studied D-MWMRN with arbitrary number of relays serving users randomly distributed in an area. Uncoordinated transmission is employed in MAC phase of the networks. We proposed IDM algorithm incorporated into *graph-based* SIC to boost the throughput performances. The superiority of the proposed technique in terms of PLR and throughput performances was demonstrated. In BC phase, the proposed joint decoding strategy in MWMRN-2C was generalized for arbitrary number of relays by introducing *VN* decoder. We also evaluated the practical optimal number of relays in D-MWMRN. It was shown that D-MWMRN with $Q = 2$ relays is the most advantageous scenario, because significant gain in terms of BER and throughput performances are achieved in low SNR environment. However, when SNR is high, D-MWMRN with $Q = 1$ relay is the best scenario to achieve maximum throughput performance with less complexity.

Chapter 6

Conclusions and Future Works

6.1 Conclusions

In this thesis, we have intensively investigated MWRN employing uncoordinated transmission strategy for future networks serving massive number of users. The main contributions of this thesis lies on the employment of the IDM algorithm in SIC to effectively decode all messages transmitted uncoordinatedly by all users, yielding remarkably throughput improvement. Moreover, the case of multiple relays considered for MWMRN was also investigated. For this, we proposed a general joint decoding and confirmed its superiority in providing BER and throughput performances gain for MWMRN with uncoordinated transmission.

We started the research by introducing uncoordinated transmission notion for MWRSN in **Chapter 4**. This chapter considered very simple setup of MWRN, where massive number of users expect to exchange information among themselves via only a single relay. Graph-based SIC is exploited to decode the messages transmitted in uncoordinated fashion. Moreover, we proposed IDM algorithm to be incorporated into graph-based SIC to increase the probability of successful decoding. It has been shown that MWSRN adopting uncoordinated transmission can be regarded as a coding structure resembling LDPC codes. Hence, the similar analysis technique, EXIT analysis, is utilized to analyze the decoding convergence behavior of the networks. We derived EXIT functions representing the evolution of iterative decoding processes in SIC and plot them into EXIT chart to visualize the decoding convergence. EXIT chart area theorem is then utilized to derive the network capacity bound of the MWSRN. It was confirmed that the proposed

MWSRN provides higher bound, which is almost two times higher compared to the MWSRN employing the conventional CSA (without IDM algorithm). A series of computer simulations were conducted to evaluate the MWSRN performances. The results showed the superiority of the proposed techniques in terms of PLR, throughput, and BER performances.

In **Chapter 5**, more general cases of MWRN, where multiple relays are employed, are investigated. In particular, two scenarios of MWMRN are considered. In the first scenario, two relays are employed to serve massive number of users divided into two clusters. The users are allowed to transmit their information uncoordinatedly in MAC phase. Since the messages are sent from the same source, the decoded messages in both relays are correlated. We introduced MI-based joint decoding strategy in the final destinations by exploiting the source correlation of the messages to enhance the networks performances. In the second scenario, we investigated D-MWMRN with arbitrary number of relays to serve distributed users. Graph-based SIC with IDM algorithm was proposed to significantly improve the networks throughput performances in MAC phase. Based on computer simulation results we confirmed that the proposed decoding strategy outperforms the conventional technique in terms of PLR and throughput performances. In the BC phase, we generalized the final joint decoding based on MI for arbitrary number of relays in D-MWMRN. It was shown that the proposed techniques in both MAC and BC phases provide significant contributions to networks performances improvements in terms of PLR, throughput, and BER. We also confirmed that $Q = \{1, 2\}$ are the practical optimal numbers of relays for D-MWMRN.

6.2 Future Works

Based on the results achieved in this thesis, we provide several insights for future works listed as follows.

- In this thesis, MWRN was analyzed and investigated over AWGN channel. It will be more interesting to investigate MWRN over Rayleigh fading channel. In this case, graph structures viewed by the relays are possibly different each others (because of independent fading), which can be further exploited using graph-based joint decoding among the relays to further enhance the performances. Moreover, it is well understood that the different channel gain

from Rayleigh fading is more beneficial for multiuser detection (MUD) technique to improve the throughput since we can exploit the capture effect in the networks.

- The decoding capability of IDM algorithm can be extended to more than *two* messages simultaneously. Employing this in graph-based SIC will boost the networks throughput of more than 2 packets/slot [24]. However, the complexity will also increase, which is very interesting topic for practical applications.

- Practically, when a user transmit its message, it will be heard not only by the relays, but also by the other users. This information can be regarded as side information, which is believed to be beneficial in the decoding process. However, how far the impacts of side information is still an interesting open problem when IDM algorithm is applied.

- Compute-and-forward (CF) relaying protocol has been theoretically proven to achieve higher sum-rate compared to the DF and AF relaying protocols. Employing CF relaying protocol in MWRN with uncoordinated transmission is very promising method to improve the total throughput of the networks.

Bibliography

[1] C. IBSG, "The internet of things: How the next evolution of the internet is changing everything," *Cisco white paper*, April 2011.

[2] Ericsson, "More than 50 billion connected devices," *Ericsson white paper*, February 2011.

[3] D. Gunduz, A. Yener, A. Goldsmith, and H. Poor, "The multiway relay channel," *Information Theory, IEEE Transactions on*, vol. 59, no. 1, pp. 51–63, Jan 2013.

[4] R. Rafie Borujeny, M. Noori, and M. Ardakani, "On the achievable rates of pairwise multiway relay channels," in *Information Theory (ISIT), 2014 IEEE International Symposium on*, June 2014, pp. 2719–2723.

[5] L. Ong, C. Kellett, and S. Johnson, "On the equal-rate capacity of the AWGN multiway relay channel," *Information Theory, IEEE Transactions on*, vol. 58, no. 9, pp. 5761–5769, Sept 2012.

[6] L. Choudhury Gagan and S. Rappaport Stephen, "Diversity ALOHA–a random access scheme for satellite communications," *Communications, IEEE Transactions on*, vol. 31, no. 3, pp. 450–457, Mar 1983.

[7] E. Casini, R. De Gaudenzi, and O. Herrero, "Contention resolution diversity slotted (aloha," *Wireless Communications, IEEE Transactions on*.

[8] G. Liva, "Graph-based analysis and optimization of contention resolution diversity slotted ALOHA," *Communications, IEEE Transactions on*, vol. 59, no. 2, pp. 477–487, February 2011.

[9] E. Paolini, G. Liva, and M. Chiani, "Coded slotted ALOHA: A graph-based method for uncoordinated multiple access," *Information Theory, IEEE Transactions on*, vol. 61, no. 12, pp. 6815–6832, Dec 2015.

[10] M. Ghanbarinejad and C. Schlegel, "Irregular repetition slotted ALOHA with multiuser detection," in *Wireless On-demand Network Systems and Services (WONS), 2013 10th Annual Conference on*, March 2013, pp. 201–205.

[11] K. Anwar and T. Matsumoto, "Three-way relaying systems using iterative spatial demapping," in *Turbo Codes and Iterative Information Processing (ISTC), 2012 7th International Symposium on*, Aug 2012, pp. 96–100.

[12] ——, "Accumulator-assisted distributed turbo codes for relay systems exploiting source-relay correlation," *Communications Letters, IEEE*, vol. 16, no. 7, pp. 1114–1117, July 2012.

[13] J. Laneman and G. Wornell, "Energy-efficient antenna sharing and relaying for wireless networks," in *Wireless Communications and Networking Confernce, 2000. WCNC. 2000 IEEE*, vol. 1, 2000, pp. 7–12 vol.1.

[14] R. Vaze and R. Heath, "On the capacity and diversity-multiplexing tradeoff of the two-way relay channel," *Information Theory, IEEE Transactions on*, vol. 57, no. 7, pp. 4219–4234, July 2011.

[15] T. Oechtering, C. Schnurr, I. Bjelakovic, and H. Boche, "Achievable rate region of a two phase bidirectional relay channel," in *Information Sciences and Systems, 2007. CISS '07. 41st Annual Conference on*, March 2007, pp. 408–413.

[16] T. Cover, "Broadcast channels," *Information Theory, IEEE Transactions on*, vol. 18, no. 1, pp. 2–14, Jan 1972.

[17] S. Pfletschinger and F. Sanzi, "Error floor removal for bit-interleaved coded modulation with iterative detection," *Wireless Communications, IEEE Transactions on*, vol. 5, no. 11, pp. 3174–3181, November 2006.

[18] K. Anwar and T. Matsumoto, "Very simple BICM-ID using repetition code and extended mapping with doped accumulator," *Wireless Personal Communications*, vol. 67, no. 3, 2012.

[19] K. Anwar, "High-dense multiway relay networks exploiting direct links as side information," in *Communications (ICC), 2015 IEEE International Conference on*, May 2016.

[20] ——, "Graph-based decoding for high-dense vehicular multiway multirelay networks," in *Vehicular Technology Conference (VTC Spring), 2016 IEEE*, May 2016.

[21] ——, "Exploiting the dynamics of rayleigh fading channels for wireless high-dense networks with multiple relays," in *General Conferences, 2016 IEICE*, March 2016.

[22] T. Helleseth, T. Klave, and V. Levenshtein, "On the information function of an error correcting code," in *Information Theory. 1997. Proceedings., 1997 IEEE International Symposium on*, Jun 1997, pp. 362–.

[23] T. Richardson and R. Urbanke, *Modern Coding Theory*. New York, NY, USA: Cambridge University Press, 2008.

[24] A. A. Purwita and K. Anwar, "Vehicular massive multiway relay networks applying graph-based random access," in *Vehicular Networking Conference (VNC), 2015 IEEE*, Nov 2015.

[25] J. Hagenauer, "The EXIT chart - introduction to extrinsic information transfer in iterative processing," in *Signal Processing Conference, 2004 12th European*, Sept 2004, pp. 1541–1548.

[26] X. He, X. Zhou, K. Anwar, and T. Matsumoto, "Wireless mesh networks allowing intra-link errors: CEO problem viewpoint," in *Information Theory and its Applications (ISITA), 2012 International Symposium on*, Oct 2012, pp. 61–65.

Achievements

1. Mohammad Nur Hasan and Khoirul Anwar, "Massive Uncoordinated Multiway Relay Networks with Simultaneous Detections", IEEE ICC 2015 - Workshop on Advanced PHY and MAC Techniques for Super Dense Wireless Networks, London, United Kingdom, June 2015 - *Refereed*

2. Khoirul Anwar and Mohammad Nur Hasan, "Uncoordinated Transmission in Multiway Relaying Systems", SCC 2015 - 10th International ITG Conference on Systems, Communications and Coding, Hamburg, Germany, February 2015 - *Refereed*

3. Mohammad Nur Hasan and Khoirul Anwar, "Joint Decoding for Multiway Multirelay Networks with Coded Random Access", 22nd Asia-Pacific Conf. on Comm. (APCC 2016), Yogyakarta, Indonesia, Aug 2016, *Under review*

4. Mohammad Nur Hasan and Khoirul Anwar, "Networked Everything Based on Massive Wireless Multiway Multirelay Networks", 2016 IEICE Techninal Report HPB, Tokyo, Feb 2016, – *Non-refereed*

5. Mohammad Nur Hasan and Khoirul Anwar, "Estimating Source Correlation Onlinve in Massive Multiway Multirely Networks", 2016 IEICE General Conference, Kyushu Japan, March 2016 - *Non-refereed*

6. Mohammad Nur Hasan and Khoirul Anwar, "Exploiting CEO Problems in Massive Multiway Multirelay Networks", 2015 38th Symposium on Information Theory and its Applications (SITA), Okayama, Japan, November 2015 - *Non-refereed*

7. Mohammad Nur Hasan and Khoirul Anwar, "Massive Uncoordinated Communications for Multi-way Relay Networks Using Iterative Demapping Algorithm", 2015 IEICE General Conference, Kusatsu (Shiga), Japan, March 2015 - *Non-refereed*

8. Mohammad Nur Hasan and Khoirul Anwar, "Capacity Bound for Uncoordinated Transmission Multiway Relay Networks", COST IC1004, Cooperative Communication for Green Smart Environments, 11th MC and Scientific Meeting, Krakow, Poland, September 2014 - *Non-refereed*